ASD-TDR-63-606

PHOTRONICS: THE GENERATION OF LIGHT IN SILICON P-N JUNCTIONS AND THE OPTICAL COUPLING OF SEMICONDUCTOR DEVICES

TECHNICAL DOCUMENTARY REPORT NO. ASD-TDR-63-606

July 1963

Electronic Technology Division
AF Avionics Laboratory
Aeronautical Systems Division
Air Force Systems Command
Wright-Patterson Air Force Base, Ohio

Project No. 4159, Task No. 415910

(Prepared under Contract No. AF 33(657)-8678
by Amelco, Inc., Mountain View, California
Author: M. A. Gilleo)

NOTICES

When Government drawings, specifications, or other data are used for any purpose other than in connection with a definitely related Government procurement operation, the United State Government thereby incurs no responsibility nor any obligation whatsoever; and the fact that the Government may have formulated, furnished, or in any way supplied the said drawings, specifications, or other data, is not to be regarded by implication or otherwise as in any manner licensing the holder or any other person or corporation, or conveying any rights or permission to manufacture, use, or sell any patented invention that may in any way be related thereto.

DDC release to OTS not authorized.

Qualified requesters may obtain copies of this report from the Defense Documentation Center (DDC), (formerly ASTIA), Arlington Hall Station, Arlington 12, Virginia.

Copies of this report should not be returned to the Aeronautical Systems Division unless return is required by security considerations, contractural obligations, or notice on a specific document.

FOREWORD

This report was prepared by Amelco, Inc., Mountain View, California, on Air Force Contract AF 33(657)-8678, under Task No. 415910 of Project No. 4159, Photronics. The work was adminstered by the Electronic Technology Division (formerly Electronic Technology Laboratory), AF Avionics Laboratory, Aeronautical Systems Division. Mr. Walter S. Chambers was project engineer for the Division.

The studies presented were begun in May 1962 and were concluded in June 1963. Dr. J. T. Last is in charge of Research and Development for Amelco, Inc.; Dr. M. A. Gilleo was responsible for the work done on this contract.

This report is the final report and it concludes the work on Contract AF 33(657)-8678.

The help of Mr. R. E. Lewis with optical technology, of Mr. O. W. Hatcher with diode production, of Mr. G. A. Lessard with device assembly, of Mr. D. G. McAllister with synthesis of the inorganic glasses, of Dr. C. S. Roberts with matters pertaining to III-V compounds, and of Mr. L. Lunn with zinc diffusion in GaAs and epitaxial growth of GaP is gratefully acknowledged. The council of Mr. W. S. Chambers of the Electronic Technology Division was valuable in determining the direction and emphasis of the work undertaken.

PHOTRONICS: THE GENERATION OF LIGHT IN SILICON P-N JUNCTIONS AND THE OPTICAL COUPLING OF SEMICONDUCTOR DEVICES

ABSTRACT

Silicon p-n junctions coupled by a light pipe were evaluated as a means for the generation, transmission, and reception of photons which would serve to transfer an electrical signal from one circuit to another without electrical interconnection. The reverse-current radiation of these junctions ranged from > 3 eV to < 0.5 eV with a maximum at about 0.56 eV. The best internal efficiency observed was about $2.5 \cdot 10^{-4}$ photon per electron for a p^+-n diode made on 1.2-ohm-cm silicon. The forward-current radiation was produced with the best efficiency in an n^+-p diode made on 0.05-ohm-cm silicon which yielded about $6.1 \cdot 10^{-4}$ photons per electron. The radiation has a maximum at about 1.1 eV with a width of a few tenths of an eV at room temperature. On a power basis the forward-current radiation is produced with about two orders of magnitude greater efficiency than reverse-current radiation. Additional data were obtained with double-injection diodes. The optical interconnection of semiconductor circuits by means of light pipes made of inorganic glasses with a high refractive index was investigated. Light-coupled transducers were constructed with diodes and with phototransistors. An optically actuated microcircuit flip-flop was assembled with an arsenic trisulfide light pipe and a gallium arsenide light source.

CONTENTS

1. INTRODUCTION. 1

2. P-N-JUNCTION LIGHT SOURCES 5

Radiative and Non-Radiative Recombination . . . 5

Light Production in Planar, Diffused Diodes . . . 12

Double-Injection Diodes 42

3. OPTICAL COUPLING OF CIRCUIT ELEMENTS . . . 59

The Theory of Light-Pipe Performance 60

The Techniques and Materials of Optical Transfer . 75

High-Refractive-Index, Inorganic, Cement Glasses . 83

4. LIGHT-COUPLED DEVICES 90

Transducers 90

An Optically-Actuated Flip-Flop 94

5. EPITAXIAL LIGHT SOURCES 100

6. CONCLUSIONS AND RECOMMENDATIONS 103

FIGURES

1. The geometry of the XLD-3 planar-diffused diode. 13

2. The light produced by an XLD-3(100dp .25) diode operated on reverse current as seen through an infrared image converter with an overall magnification of about 85X. 15

3. The light produced by an XLD-3(100dn .068) diode operated on forward current as seen through an infrared image converter with an overall magnification of about 85X. 17

4. Light output and voltage drop vs reverse current through an XLD-3(100dn .068) diode. 22

5. Light output and voltage drop vs forward current through an XLD-3(100dn .068) diode. 31

6. Junction capacitance vs applied reverse-bias voltage for XLD-3(100dn .068) diodes with an undiffused (predeposited) junction and with junctions diffused for 1/4 and 1 hour at 1200°C. 34

7. The dimensions of an XLD-1(40x200) double-injection diode (not to scale). 45

8. Light output as a function of slit position across an XLD-1(40x200) operated at 9.2A forward current. 47

9. The radiation from an XLD-1(40x200) 1280, 4 double-injection diode as seen through an infrared image converter with an overall magnification of about 85X. . . . 48

10. The negative-resistance in the V-I characteristic of XLD-1(40x200) gold-doped at 1010° C is shown by these facsimiles of oscilloscope traces (a) 10 V/div (vertical), 5 microsec-div (horizontal), (b) 20 mA/div, 5 microsec/div. 53

11. Light output (in terms of 7102 anode current) and voltage drop vs forward current through XLD-2(4x200)1280, 4. 55

12. Light output (in terms of 7102 anode current) and voltage drop vs forward current through XLD-1(-25x200). 57

13. The path of light from a source in medium i of refractive index n_i to a point in medium r with refractive index n_r. 63

14. The path of light from a source in medium i with a refractive index n_i into a light pipe of index n_r immersed in a medium of unit index. 65

15. A plot of $d\phi_{\parallel}(r)/dr$ and $\phi_{\parallel}(r)$ vs r for a medium r with $n_r = 1.84$ and a source medium i with $n_i = 3.56$. 66

16. A plot of $d\phi_{\perp}(r)/dr$ and $\phi_{\perp}(r)$ vs $\underline{r}$ for a medium $\underline{r}$ with $\underline{n}_{\underline{r}} = 1.84$ and a source medium $\underline{i}$ with $\underline{n}_{\underline{i}} = 3.56$. 67

17. A plot of $d\phi_{\parallel}(r)/dr$ and $\phi_{\parallel}(r)$ vs $\underline{r}$ for a medium $\underline{r}$ with $\underline{n}_{\underline{r}} = 2.47$ and a source medium $\underline{i}$ with $\underline{n}_{\underline{i}} = 3.56$. 68

18. A plot of $d\phi_{\perp}(r)/dr$ and $\phi_{\perp}(r)$ vs $\underline{r}$ for a medium $\underline{r}$ with $\underline{n}_{\underline{r}} = 2.47$ and a source medium $\underline{i}$ with $\underline{n}_{\underline{i}} = 3.56$. 69

19. The light flux available from a source in a medium with $\underline{n}_{\underline{i}} = 3.56$ over 2π steradians in medium $\underline{r}$ with index $\underline{n}_{\underline{r}}$ and from a light pipe of index $\underline{n}_{\underline{r}}$ immersed in a medium of unit refractive index as a fundtion of $\underline{n}_{\underline{r}}$. . . . 71

20. The exit of light from a medium $\underline{i}$ of index $\underline{n}_{\underline{i}}$ through a thick layer of index $\underline{n}_1$ into an external medium 2 of index $\underline{n}_2$ where $\underline{n}_{\underline{i}} > \underline{n}_1 > \underline{n}_2$. 73

21. A laminar-optical light-pipe horn. 80

22. Collimation within the length of a type-A horn for various angles of incidence at the entrance to the horn. . . 82

23. An illustration of the escape condition for a ray which enters the side of a horn in a symmetrical light-guide system with type-A horns. 84

24. The escape condition for a ray in a light guide with a type-B horn ending. 84

25. The phase diagram of the As-S-Br system shows the glass-forming region, softening points in °C, and some indices of refraction. 87

26. The phase diagram of the As-S-I system shows the glass forming regions, [55] softening points in °C, [55] and indices of refraction. 88

27. Output current vs forward input current for light-coupled transducer No. 4 with a 30-mil-diam light pipe of IR 20. 94

28. Output current vs reverse input current for light-coupled transducer No. 4 with a 30-mil-diam light pipe of IR 20. 95

29. A photomicrograph of a microcircuit flip-flop at about 135X magnification with the location of the 12-mil-diameter light pipe shown. 98

30. The opto-electronic circuit with a microcircuit flip-flop which was arranged for optical actuation by means of light through a light pipe from a GaAs diode in a second, electrically-isolated circuit. 99

1. INTRODUCTION

The objectives of the work being reported are to achieve the optimum means for the production, transmission, and reception of photons so that the transfer of electrical signals by means of photons may be efficiently accomplished. In this way photons can serve to interconnect two or more circuits in such a way as to accomplish electronic functions such as switching, logical operations, impedance transformation, and modulated signal transfer; no electrical interconnection of the circuits need exist.

A p-n junction in a semiconductor provides conditions admirably suited both to the emission and to the detection of photons. The p and n regions may, for simplicity, be regarded as sources of holes and electrons respectively. Without application of an external potential between the p and n regions there is no net transfer of charge carriers between the two regions because the potential energy for holes and electrons is at a minimum for each in its respective region of origin.

In the case of absorption of a photon in the p-n junction, the electron-hole pair thus created will separate; each charge carrier of this pair then diffuses to the region where its potential energy is lowest. In this way a photovoltaic current is generated.

Conversely, a potential (forward) may be applied to the p-n junction with the p region positive with respect to the n region so that electrons flow into the p region and holes into the n region. Then in

---

Manuscript released by the author July 1963 for publication as an ASD Technical Documentary Report.

each region the minority carriers thus injected will recombine, usually at an impurity atom, with probability that a photon with an energy less (approximately by the impurity ionization energy) than that of the semiconductor band gap will be emitted.

Alternatively, a potential (reverse) may be applied to the p-n junction such that the minority-carrier electrons in the p region travel to the n region and vice versa. A much larger potential difference is necessary to accomplish this so that the charge carriers may acquire kinetic energy, may create further charge carriers by ionization processes, and may recombine to yield radiation of energy greater than that of the band gap.

When the holes become heated, as in the case of reverse-current operation of a p-n junction, those holes with the highest kinetic energy may occupy a higher-energy (lower-lying) valence band. In this case a hole which makes a transition to a lower-energy valence band (intraband transition) will emit radiation, and analogously for hot electrons.

The p-n junction therefore provides us with a means for the detection of radiation and with at least three different mechanisms for the generation of radiation by the flow of current. An important problem which remains is that of transferring the radiation from the source junction to the receiving junction.

In a light-coupled transducer the input signal generates light which is converted into an electrical output signal by the detector. For

most efficient operation all of the light generated would be conveyed to the receiver. Because of the high index of refraction of semiconductor materials only a few percent of the light generated may escape into the air and, likewise, much of that incident from the air is reflected so that little may enter. Therefore, a light pipe made of a transparent material with an index of refraction approaching that of the semiconductor is needed to achieve efficient current transfer in a light-coupled transducer.

For an investigation of the means for achieving the optical interconnection of circuits and the attendant problems described above, silicon was selected as the principal semiconductor material for the fabrication of light sources and receivers. Silicon technology has become quite advanced as a consequence of its extensive use in transistors and microcircuits. Accordingly, an extension of its use to optical interconnection of circuits would be logical and advantageous.

Although the photovoltaic effect in silicon p-n junctions has been brought to an advanced state, the generation of radiation by the flow of current through p-n junctions in silicon is not yet completely understood. Therefore, much attention was devoted to the generation of radiation by reverse-current flow in silicon p-n junctions, which is the most interesting and perhaps least understood mechanism, and to radiation produced by forward-current flow. The objective of this research was to gain greater understanding and more quantative knowledge of these processes so that more efficient production of radiation could be achieved. For this purpose

p-n junctions were formed in base materials of silicon of p and n type with a wide range of resistivities. The radiation produced by these junctions was measured and evaluated in terms of existing theories pertaining to this radiation.

The problem of the optical coupling which can be achieved between a source and receiver immersed in separate pieces of a material of high refractive index by means of a light pipe was examined theoretically. Experiments were made in which light pipes with several refractive indices which approach that of silicon were used and the results compared with the theory. The devices used in these experiments were light-coupled transducers and the current-transfer coefficient of these transducers was used as a measure of the optical coupling achieved.

As a demonstration of an application of optical coupling in solid-state circuitry the input transistor of a microcircuit flip-flop made on silicon was connected by a light pipe to a light-source diode. In this way the flip-flop could be triggered by a current in a circuit not electrically connected to the flip-flop circuit.

The theoretical and experimental background which has been established by previous workers in this field is presented in subsequent sections of this report. The quantitative data which were obtained in the experiments conducted to provide information pertinent to the problems described above are also presented together with their interpretation and application to the solution of the problems.

2. P-N-JUNCTION LIGHT SOURCES

Radiative and Non-Radiative Recombination

The production of light by recombination of the charge carriers in a semiconductor containing a p-n junction has been mentioned as a promising means for use in photronics. Such light was first reported by Haynes and Briggs[1] for a junction in germanium. Subsequently it was investigated by others in various materials. The work of particular interest is that on Si by Haynes and Westphal[2] and by Chynoweth and McKay.[3]

An important result of Chynoweth and McKay for silicon, from the point of view of its application to photronics, is that only about one in 10^3 to 10^4 electrons traversing the p-n junction in the forward direction gives rise to a photon; most recombination processes are non-radiative. This poor efficiency arises for the following reasons, among others. It has been shown by Herman[4] that germanium and silicon have such an energy-band structure that direct transitions (those not involving a change of momentum) involve a higher energy than indirect transitions. For the energy-band structure of germanium and silicon

---

[1] J. R. Haynes and H. B. Briggs, Phys. Rev. 86, 647 (1952).

[2] J. R. Haynes and W. C. Westphal, Phys. Rev. 101, 1676 (1956).

[3] A. G. Chynoweth and K. G. McKay, Phys. Rev. 102, 369 (1956).

[4] F. Herman, Phys. Rev. 93, 1214 (1954); ibid. 95, 847 (1954); Proc. Inst. Radio Engrs. 43, 1703 (1955).

Dumke[5] has calculated the radiative-recombination lifetime for intrinsic material to be about 2 and $2 \cdot 10^4$ sec, respectively, for indirect transitions. In germanium the direct radiative-recombination lifetime is about 0.3 sec; no such radiation is to be expected from silicon. However, intrinsic material of such high perfection that these radiative-recombination lifetimes would dominate would be difficult to realize.

When intrinsic radiation is produced in silicon by the recombination of electrons at the conduction-band minima with holes at the valence-band maximum the crystal momentum is conserved by the absorption or emission of phonons. In both silicon and germanium there are four branches to the phonon spectrum in the direction of conduction-band minima. Consequently, there are available four phonons of different energy each of which has the required crystal momentum necessary to the recombination transition. By careful observation of the intrinsic radiation of silicon and germanium Haynes et al.[6] have identified the effect of longitudinal and transverse phonons of the optical and acoustic branches of the phonon spectrum.

---

[5] W. P. Dumke, Phys. Rev. 105, 139 (1957).

[6] J. R. Haynes, M. Lax, and W. F. Flood, J. Phys. Chem. Solids 8, 392 (1959).

At low temperatures for which the thermal dissociation of excitons (coupled electrons and holes) is small the radiation arises predominantly from recombination of excitons with the emission of a transverse optical phonon in intrinsic silicon. The recombination rate of free electrons and holes was found to be 1/6 of the exciton recombination rate at 83°K by Haynes et al.[7]

In less pure material recombination most probably takes place at impurity atoms in an Auger-type process involving either two like or two unlike charge carriers and a trap, as has been shown by Bess.[8] The process involving a trap and unlike charge carriers turns out to be the most probable one. In this process a free hole, for example, approaches a trap filled with an electron and with a free electron in the neighborhood. A transition is then possible in which the hole annihilates one of the electrons and the other electron is ejected into the conduction band with a kinetic energy equal to any excess of energy present. The probability that a photon will be emitted in the recombination process turns out to be very small. The energy of a photon produced in this way will be less than the band-gap energy of the semiconductor by the energy of ionization of the impurity atom to first approximation.[2] Therefore,

---

[7] J. R. Haynes, M. Lax, and W. F. Flood, Proc. of the Int. Conf. of Semicond. Phys., Prague, 1960 (Academic Press, New York, 1961), p. 423.

[8] L. Bess, Phys. Rev. 105, 1469 (1957).

non-radiative recombination processes dominate. For Ge Bess found that the radiative lifetime would be about 300 times greater than the non-radiative lifetime. For silicon the situation is much poorer. However, Bess also showed that the conditions most favorable to radiative recombination occurred for impurity-concentration ratios about a factor of ten from the compensation point.

The addition of impurities to silicon has been shown to give rise to an electronic complex which results in further radiative processes as has been shown by Haynes.[9] In the case of an n-type impurity Haynes has shown that the complex consists of a hole bound to a positive donor by an electron-pair bond. Similarly, in the case of a p-type impurity the complex is obtained by a reversal of the sign of the charges, i.e. an electron bound to a negative acceptor by a hole-pair bond. Radiation from these complexes consists of very narrow lines (width < 0.0005 eV) because the recombining electron and hole are both immobilized. The radiative recombination occurs with and without emission of a transverse optical phonon. The dissociation energies of these complexes is about one tenth of the ionization energy of the impurities so that this mechanism for the production of radiation would only be important at temperatures much below room temperature.

---

[9] J. R. Haynes, Phys. Rev. Letters 4, 361 (1960).

These above considerations are primarily applicable to p-n junctions which carry a current in the forward direction, i.e. to minority-carrier recombination. A comparable understanding of the processes of recombination in the microplasmas reported Chynoweth and McKay[3] in reverse-biased, silicon, p-n junctions has not yet been achieved because of the greater difficulty of the problem. However, the response time for the light from a reverse-biased junction is much faster than that of a forward-biased one because we are dealing with a majority-carrier-recombination lifetime (time of the order of $\rho\epsilon$, the product of bulk resistivity and permittivity) rather than with a minority-carrier-recombination lifetime.

The charge carriers are subject to higher electric fields than in the case of forward-current operation where voltages of 0.5 to 0.7 V are sufficient for the onset of a substantial forward current. In the reverse direction, however, the voltage must be considerably higher. Chynoweth and McKay[10] have shown that the threshold energy for electron-hole-pair production in silicon is 2.25 eV. Moreover, they have also shown that for reverse voltages less than about six volts the principal current can be attributed to field emission at the junction rather than to the

---

[10] A. G. Chynoweth and K. G. McKay, Phys. Rev. 108, 29 (1957).

formation of microplasmas at the junction.[11] Consequently, at breakdown voltages below about six volts the character of the light produced by the junction changes.

As a consequence of the larger potential differences across the junction, the charge carriers acquire a substantial kinetic energy. Therefore, upon recombination the energy available from the charge carriers is greater than the band gap of the semiconductor. Accordingly, the spectral distribution of the radiation shows an extension toward shorter wavelengths. The upper energy limit corresponds at room temperature to the sum of the band-gap energy of 1.09 eV and the pair formation energy of 2.25 eV or about 3.34 eV; the probability of a recombination between energetic holes and electrons, which would be required to achieve higher photon energy, is negligibly small. The probability of kinetic energies in excess of 2.25 eV is also small because charge carriers with an energy above this value quickly lose it to pair formation.

As a further consequence of the high kinetic energy attained by the charge carriers which carry the reverse current, their temperature is much higher than that of the lattice. At a sufficiently high temperature the holes may undergo an intraband transition (a transition between

---

[11] A. G. Chynoweth and K. G. McKay, Phys. Rev. 106, 418 (1957).

valence bands) with the emission of light. The intraband-transition radiation of hot holes in germanium was first observed by Chynoweth and Gummel[12] and interpreted theoretically by Wolff.[13] Radiation which it is believed may be attributed to intraband transitions of hot holes has been observed in silicon.[14] However, the intraband-transition radiation in silicon occurred at a longer wavelength than the band edge whereas in germanium it was observed at a wavelength shorter than that of the band edge. In both cases the radiation attributed to the intraband-transitions of holes was the strongest component present.

The experimental investigation of the generation of light in silicon p-n junctions was carried out in three categories. In the first category planar, diffused, p^+-n and n^+-p junctions in silicon were used. With these diodes the efficiency of the production of light was examined as a function of the resistivity of the base materials and the extent of diffusion of the junction. Forward and reverse current was used and the spectral region from 0.3 to 3 microns was observed. In the second category an examination was made of the recombination of electrons or holes in indium-doped silicon at low temperatures. The recombination process of

---

[12] A. G. Chynoweth and H. K. Gummel, J. Phys. Chem. Solids 16, 191 (1960).

[13] P. A. Wolff, J. Phys. Chem. Solids 16, 184 (1960).

[14] A. G. Chynoweth (private communication). The presence of such radiation had been postulated earlier by Chynoweth and McKay.[3]

electrons with holes at un-ionized indium had been reported by Pokrovsky and Svistunova[15] to take place with nearly unit quantum efficiency below 80°K. In the third category diodes of the double-injection kind ($\underline{p}^+$-$\underline{i}$-$\underline{n}^+$) were used to study the recombination of electrons and holes of comparable number density in a relatively pure region. Also with double-injection diodes it was possible to observe separately the recombination radiation of holes in an $\underline{n}^+$ region and electrons in a $\underline{p}^+$ region.

Light Production in Planar, Diffused Diodes

A planar, diffused diode was designed (Fig. 1) which would leave most of the diffused area (the junction area) bare so that most of the light generated would escape. At the same time the aluminum film which was used to make contact with the diffused area was designed to minimize the voltage drop as a consequence of surface resistivity so that a very high current density could be achieved over the area of the junction. The area of the aluminum to which contact is made with thermo-compression-welded, gold wires was taken outside of the junction area over the silicon oxide so that a light pipe could be placed in intimate contact with the whole area of the junction. Some of those diodes which were used with light pipes had no oxide over the diffused area except at its perimeter where the oxide served as protection. Those diodes used without light pipes

---

[15] Y. E. Pokrovsky and K. J. Svistunova, J. Phys. Chem. Solids 22, 39 (1961).

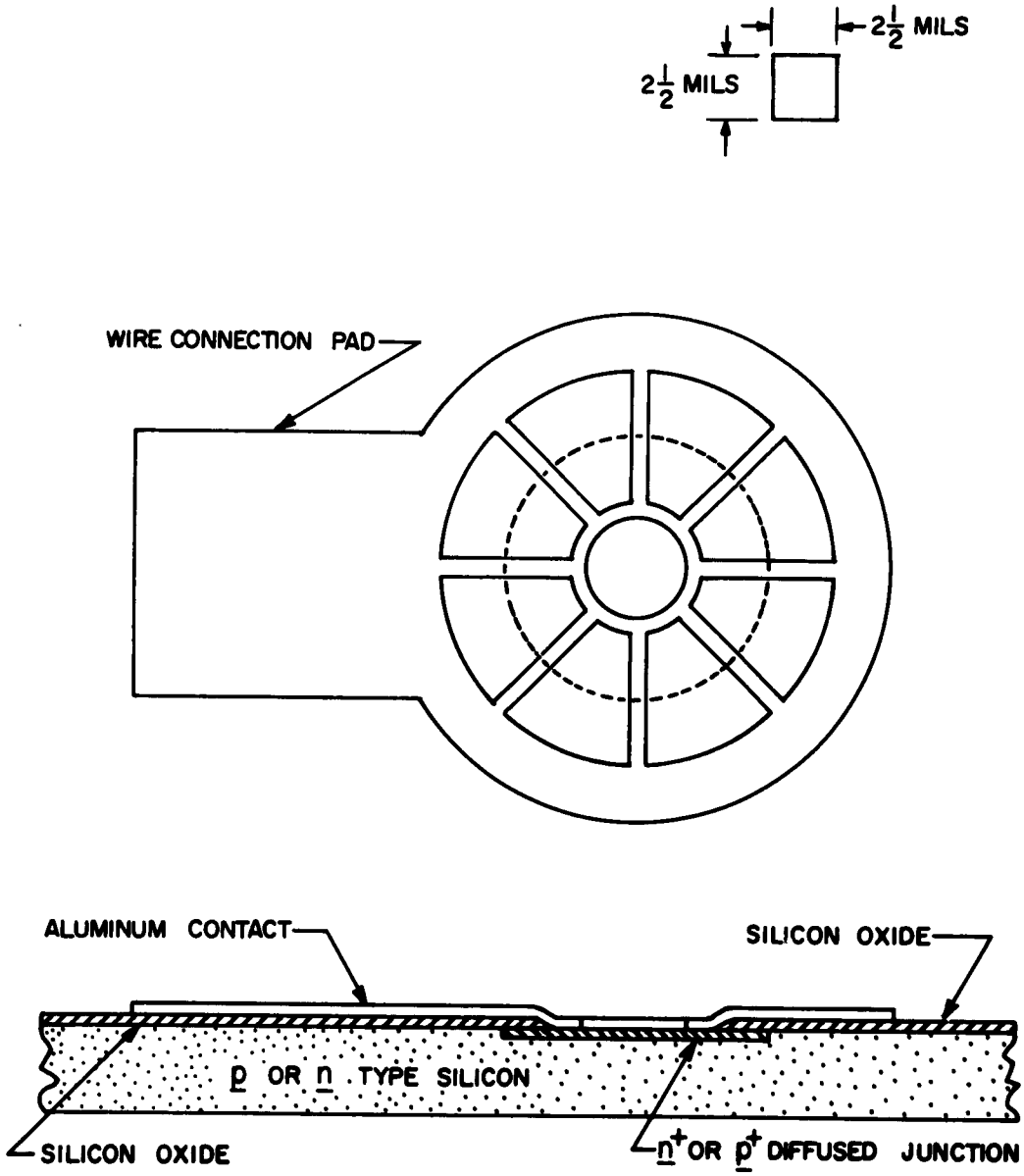

Fig. 1. The geometry of the XLD-3 planar-diffused diode.

were always oxide covered except under the aluminum. The diodes were mounted on TO-5-size headers for use in measurement of light output as a function of the magnitude and direction of the current.

An examination was made of the light output of an XLD-3(100dp.25) diode (here the 100d in parentheses indicates a diffused area of 100 ten-thousandths of an inch in diameter and p. 25 indicates that the diode was formed on 0.25-ohm-cm, p-type silicon) with forward and reverse current by means of an infrared image converter. As would be expected, it was found that with reverse current the junction perimeter was brightly lighted with the area of the junction also lighted but much more faintly. Under about 85X magnification no bright spots could be seen either on the perimeter or over the area of the junction when it was operated with 2.5 microsec pulses of 0.48 A (Fig. 2). However, when a direct current of about 10 ma was used the junction was a ring of bright spots while the area was dark (Fig. 2).

With forward-current consisting of 2.5 microsec pulses of 1 A the whole area of the junction was brightly lighted with somewhat greater brightness at the junction perimeter. In addition appreciable light could be seen outside of the junction and even outside of the outer aluminum ring (Fig. 1). It is believed that the light is being carried by multiple internal reflection in the silicon oxide because imperfections in the oxide have been seen to cast shadows as if the light were proceeding radially outward.

(a) (b) (c)

Fig. 2. The light produced by an XLD-3(100dp . 25) diode operated on reverse current as seen through an infrared image converter with an overall magnification of about 85X. (a) The diode with external illumination. (b) Junction radiation with 0.48 A pulses 2.5 microsec long; about $2.4 \cdot 10^6$ pulses were used for a total duration of 6 sec. (c) Junction radiation with about 10 mA d-c reverse current for 60 sec.

Later photographs of light from a XLD-3(100dn .068) diode showed the effect of the oxide more clearly. A good, clear oxide showed less scattered light (Fig. 3) than a poor, roughened one. Also in this case the light was brighter near the aluminum spokes, presumably because the lower series surface resistance allowed a greater current density near the electrodes. It is possible that the oxide may carry away a significant portion of the light produced by the diode.

A series of measurements was made with these diodes with an RCA 7102 photomultiplier with an S-1 infrared-sensitive photocathode and with an Eastman Kodak Type Q-1 PbS cell with a 4 x 4 mm area. With the 7102 the magnitude of the forward-current radiation at about 1.15 microns and the time constants τ_b for the build-up and τ_d for the decay of the radiation could be evaluated. Also the reverse-current radiation for $\lambda < 1.2$ microns could be evaluated. In conjunction with a sharp-cut-off, long-wavelength-pass interference filter which reduced radiation at 1.6 microns to 5% or less, the PbS cell could be used to evaluate the the fraction of the total radiation for $\lambda > 1.6$ microns which would be most probably intraband-transition radiation.[14]

The 7102 photomultiplier was calibrated for sensitivity at 1.1 microns by means of a tungsten lamp and an interference filter. The lamp had been calibrated for a color temperature of 2854°K by the National Bureau of Standards; the transmission-vs-wavelength curve of the interference filter was used to calculate the spectral power which reached the photocathode. The light intensity was measured in foot

(a) (b)

Fig. 3. The light produced by an XLD-3(100dn .068) diode operated on forward current as seen through an infrared image converter with an overall magnification of about 85X. (a) The diode with external illumination. (b) Junction radiation with 100 microsec pulses at 3 A current; about $4 \cdot 10^3$ pulses were used for a total duration of 0.4 sec.

candles with a Weston Model 756 Foot-Candle Meter. The result was 142 electrons on the average at the anode per photon at the cathode at 1.1 microns wavelength with a precision estimated to be ± 20%.

Reverse-Current Radiation

The reverse-current radiation, as the data (Table I and II) show, is little affected by the resistivity of the base material and the gradient at the junction. The radiative build-up and decay times were always less than the 5-nanosec resolution time of the 7102 photomultiplier and the associated Tektronix Model 581 oscilloscope. These observations are consistent with the microplasma model of Chynoweth and McKay[3] and with that of Rose.[16]

Previously, however, it has not been explicitly shown that the effect of minority-carrier lifetime is inconsequential to the decay time for reverse-current radiation. Also it has been shown that with a 50-ohm source impedance the rise as well as the decay times for reverse-current radiation can be made less than 5 nanosec. The experiments of Senitzky and Moll[17] indicated that this would be the case provided that the RC time constant of the junction capacitance and source impedance were sufficiently small.

---

[16] D. J. Rose, Phys. Rev. 105, 413 (1957).

[17] B. Senitzky and J. L. Moll, Phys. Rev. 110, 612 (1958).

Table I. The radiative efficiency of p^+-n-type, silicon diodes.

Resistivity of Base Material (ohm-cm)	Diffusion (°C, h)	Breakdown Voltage (volts)	Forward Current			Reverse Current	
			Photons[a] / Electron	Percent Radiation $\lambda > 1.6\mu$	Radiative Lifetime (nanosec)	Photons[a] / Electron	Percent Radiation $\lambda > 1.6\mu$
1.2	-	22	$1.9 \cdot 10^{-6}$	≤ 0.6	210	$3.9 \cdot 10^{-6}$	61
0.3	-	17	$2.7 \cdot 10^{-6}$	~ 0	280	$3.6 \cdot 10^{-6}$	44
0.075	-	11	$8.0 \cdot 10^{-6}$	0.2	635	$1.8 \cdot 10^{-6}$	41
0.075	1200, $\frac{1}{4}$	12	$5.5 \cdot 10^{-6}$	≤ 0.25[b]	250	$2.8 \cdot 10^{-6}$	62
0.075	1200, 1	19	$4.1 \cdot 10^{-6}$	≤ 0.4	270	$2.7 \cdot 10^{-6}$	52
0.068	-	8	$7.5 \cdot 10^{-6}$	≤ 0.5	460	$1.9 \cdot 10^{-6}$	46
0.068	1200, $\frac{1}{4}$	17	$6.7 \cdot 10^{-6}$	≤ 0.3	350	$2.8 \cdot 10^{-6}$	48
0.068	1200, 1	23	$5.7 \cdot 10^{-6}$	1.8	400	$2.7 \cdot 10^{-6}$	46
0.013	-	4	$3.2 \cdot 10^{-6}$	0.2	155	$2.8 \cdot 10^{-7}$	34

a These data apply to the photon flux in air on one side (2π steradians) of the diode; to obtain the total internal flux over 4π steradians multiply by 65 to allow for internal reflections and for emission over all angles.

b The $\leq$ sign indicates that the undetected radiation could be as large as the figure given which represents the noise level.

Table II. The radiative efficiency of n^+-p-type, silicon diodes.

Resistivity of Base Material (ohm-cm)	Diffusion (°C, h)	Breakdown Voltage (volts)	Forward Current			Reverse Current	
			Photons[a] / Electron	Percent Radiation $\lambda > 1.6\mu$	Radiative Lifetime (nanosec)	Photons[a] / Electron	Percent Radiation $\lambda > 1.6\mu$
1.5	-	32	$2.1 \cdot 10^{-6}$	7.6	510	$2.4 \cdot 10^{-6}$	64
0.25	-	17	$4.6 \cdot 10^{-6}$	~ 0.5	460	$1.9 \cdot 10^{-6}$	55
0.25	1200, $\frac{1}{4}$	22	$5.0 \cdot 10^{-6}$	0.6	400	$2.0 \cdot 10^{-6}$	60
0.25	1200, 1	26	$5.7 \cdot 10^{-6}$	2.3	400	$2.5 \cdot 10^{-6}$	56
0.05	-	9	$9.4 \cdot 10^{-6}$	$\simeq 0.2$	320	$8.8 \cdot 10^{-7}$	45
0.012	-	5.7	$9.9 \cdot 10^{-7}$	≤ 1.5	44	$2.7 \cdot 10^{-7}$	37
0.0087	-	5	$4.6 \cdot 10^{-7}$	≤ 2.7	-	$2.2 \cdot 10^{-7}$	36

[a] These data apply to the photon flux in air on one side (2π steradians) of the diode; to obtain the total internal flux over 4π steradians multiply by 65 to allow for internal reflections and for emission over all angles.

[b] The $\leq$ sign indicates that the undetected radiation could be as large as the figure given which represents the noise level.

A typical plot of light output and voltage drop vs current (Fig. 4) shows a nearly linear variation of light with current from 200 to nearly 5000 A cm^{-2} (the diode area is $5.08 \cdot 10^{-3}$ cm^2). The voltage drop varies in this case about as

$$V = 11.6 + 6.7I$$

which indicates that the diode has a breakdown voltage with a high-current pulse of 11.6V and a series resistance of 6.7 ohms. The voltage drop and breakdown voltage tend to differ as the rise time of the pulse voltage varies. The breakdown voltage observed tended to be lower as the rise time was slower: The E-H 132A pulse generator had about a 12-nanosec rise time, the 16-microsec pulse-forming-network (PFN) had about a 5-microsec rise time. On a curve tracer (Tektronix Model 175) the breakdown voltage was about 7V at 0.02 mA. It may be that a rapid rate of rise of the voltage across the junction leads to the initiation of a larger number of microplasmas than a slower rate. Many of these microplasmas may lie in a region of higher breakdown voltage but do not extinguish once ignited so that the voltage drop remains high.

With currents above 1 A the apparent resistance dropped to about 3.4 ohms. With a planar-diffused diode the initial breakdown takes place near the surface where the impurity gradient is higher. When the voltage drop in the series surface resistance becomes high enough, the potential at the bottom of the diffused area reaches breakdown (with pulses having a slow rate of rise) also so that the series resistance is decreased.

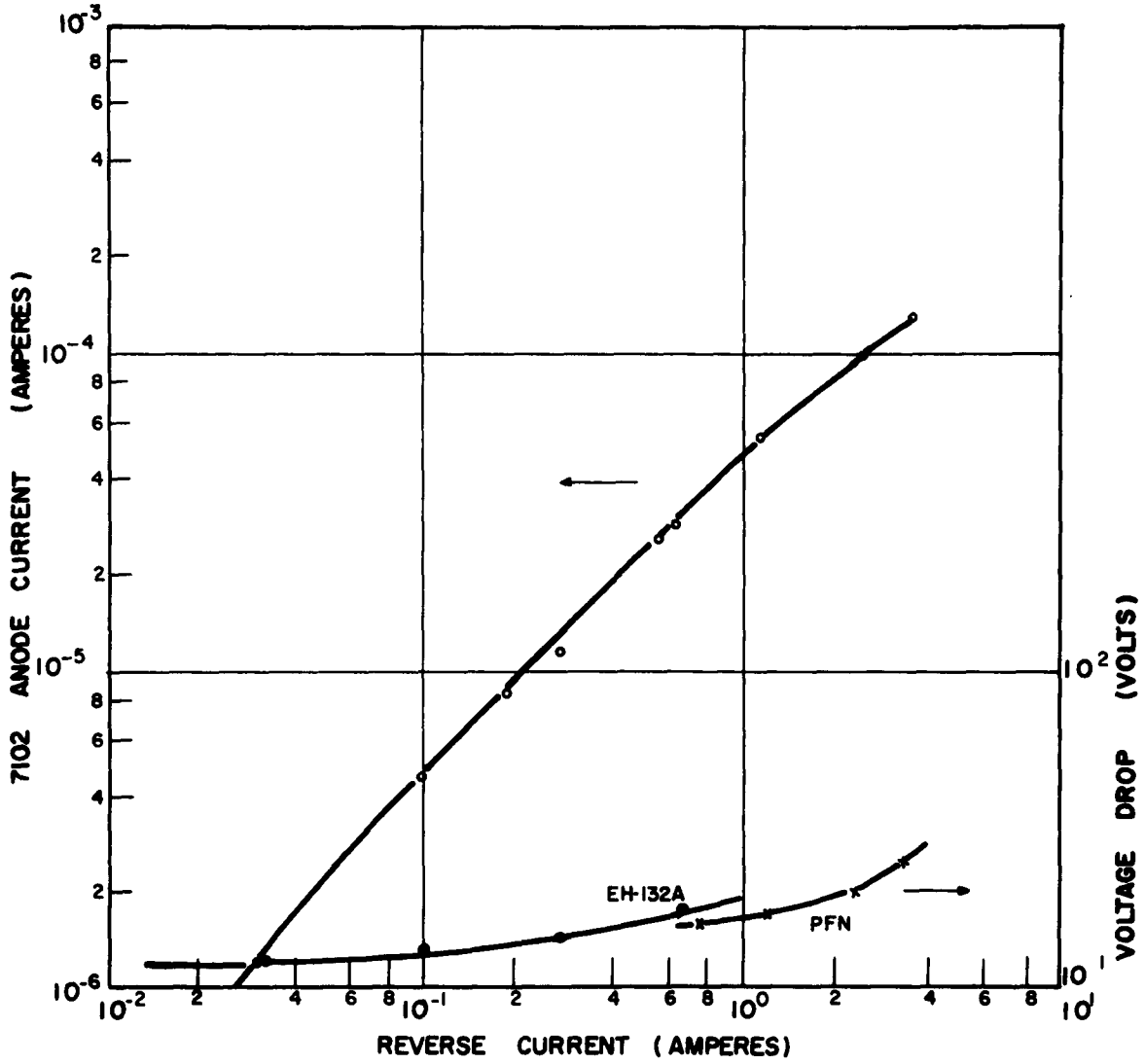

Fig. 4. Light output and voltage drop vs reverse current through an XLD-3(100dn .068) diode. The light output is given in terms of the 7102 photomultiplier anode current. The E-H-132A rise time is 12 nanosec and that of the PFN is 5 microsec.

Usually at voltage drops considerably above the breakdown voltage the junction becomes heated intensely at some spot on the surface and the device is mechanically damaged by a spark; at this point the measurements are terminated.

The radiation produced by a junction operated on reverse current is generally several times lower in intensity (see Tables I and II) than the forward-current radiation on a per-unit-current basis. The principal component of reverse-current radiation lies in the region of 2 microns according to Chynoweth.[14] By the use of a variety of filter glasses it was found that the peak lies at about 2.2 microns. This radiation is not of thermal origin because it has been found that with the XLD-3(100dn. 068) diode, for example, the proportion of radiation at wavelengths greater than 1.6 microns remained about the same from 0.182 to 0.713 A reverse current. No detector with a time constant shorter than the 200-microsec time constant of the PbS cell was available to determine whether the long-wavelength radiation responds as quickly as the shorter-wavelength ($\lambda < 1.2$ microns) radiation produced by reverse current. The change of the proportion and magnitude of the long ($\lambda > 1.6$ microns) and short ($\lambda < 1.6$ microns) wavelength components of radiation with change in the resistivity of p-type silicon as the base material is quite different (Table II). The portion of the radiation with $\lambda > 1.6$ microns ranged from 64% with 1.5-ohm-cm, p-type silicon to 36% with 0.0087-ohm-cm, p-type silicon. From these data, it can be seen that the short-wavelength radiation decreased only about six times while the long-wavelength radiation decreased by about twenty times for the same decrease of resistivity.

It will be noted from the data (Tables I and II) that the efficiency of production of reverse-current radiation increases with increasing resistivity of the base material on a per-unit-current basis. However, the breakdown voltage also increases with the resistivity of the base material so that the efficiency is not increasing on a per-unit-power basis as the base-material resistivity increases. Moreover, it was found that the upper limit of reverse-current operation of a light-producing diode tended to fall at a lower current so that the maximum light output available from the diode tended to be lower as the base-material resistivity increased.

The optical absorption of silicon in the region of 2 microns is much smaller than in the neighborhood of the absorption edge(1.1 microns) so that the long-wavelength component of the radiation might be expected to be stronger than shorter-wavelength components. However, as the data show (Table I and II) the proportion of long-wavelength radiation is little affected by a greater depth of junction as is produced by longer diffusion. Moreover, it has been observed that the total intensity of the reverse-current radiation is little changed when observed from the other side of a ca. 100-micron-thick wafer from that in which the junction was diffused. The long-wavelength component, which is strong, is little affected.

The total amount of radiation produced within the silicon is much greater than that reported from measurements in air (Tables I and II) because of the loss by internal reflection. As will be shown later in Section 3, about 3.1% of the radiation incident on a silicon surface covered

with silicon oxide from a point source within is transmitted. In addition, the radiation reported is that measured from one side. Consequently, the efficiency in terms of photons produced per electron as tabulated must be multiplied by 65 to yield the efficiency of radiative recombination. The best efficiency observed is then of the order of 10^{-4} photons per electron for reverse current.

Forward-Current Radiation

In contrast to reverse-current radiation, forward-current radiation (Tables I and II) rises and falls with a time constant determined by the minority-carrier lifetime; the efficiency of production reaches a maximum at a specific doping level between 0.01 and 0.1 ohm cm. The radiation has a rather narrow spectrum which is centered on the absorption edge (band gap) of intrinsic silicon, or at an energy less than the band gap by the ionization energy of the impurity. The efficiency of production of forward-current radiation is several times greater than for reverse-current radiation on a per-unit-current basis. On a per-unit-power basis the efficiency for forward-current radiation may be nearly two orders of magnitude greater than for reverse-current radiation because of the smaller voltage drop.

When allowance is made for internal reflection loss and radiation in the opposite direction from the detector is taken into account, the best efficiency observed is about $5 \cdot 10^{-4}$ photons per electron. This efficiency is surprisingly high in comparison with the efficiency which would be expected on the basis of the radiative lifetime of $2 \cdot 10^{4}$ sec calculated

for silicon by Dumke;[5] with a ca. 1-microsec, radiative lifetime observed an efficiency of the order of 10^{-10} would be estimated. Therefore, the probability of radiative recombination at an impurity atom, or other recombination center, must be much greater than the intrinsic-radiative-recombination probability.

The strong effect of the base material on the production of light in forward-current operation also means that the characteristics of this light are an indication of the properties of the material. It has been found that the minority-carrier lifetime determined by the junction-recovery method[18] is in close accord (± 25%) with that determined by the rise and fall time of the light from the same junction. The forward-current used in the junction-recovery method was often one to two orders of magnitude smaller than that used in current pulses to produce an adequate light level for radiative-decay measurements. This observation has recently been confirmed by Smirnov et al.[19]

Although it would be expected that the light output would be nearly proportional to the minority-carrier lifetime if the competing decay

---

[18] Transistor Technology, Edited by F. J. Biondi (D. Van Nostrand Book Co., New York, 1958), Vol. III, p. 315.

[19] L. S. Smirnov, V. S. Vavilov, and N. N. Gerasimenko, Sov. Phys.-Solid State 4, 1927 (1963).

process were non-radiative, such behavior is not shown clearly by the data for silicon with a radiative decay time of $2 \cdot 10^4$ sec.[5] The recombination centers which reduce the minority-carrier lifetime probably also cause radiative recombination with a small probability. In addition, we must always be dealing with a variety of recombination mechanisms. Nevertheless, the poorest units in a given batch invariably exhibit the shortest radiative-decay lifetimes.

Therefore, it would be expected that substantial improvement could be achieved in the radiative efficiency for forward-current operation if an effort were made to increase the minority-carrier lifetime. However, such a goal is not usually sought in the production of diodes or transistors because of the slowness of switching that results. Consequently, a substantial change would have to be made in the procedure of processing diodes.

In an effort to "harden" the reverse characteristic of an $\underline{n}^+$-$\underline{p}$ diode on 1.5-ohm-cm material, nickel diffusion was used. The desired hardening effect was achieved without much effect on the lifetime or radiative efficiency. However, the long-wavelength component of radiation and the voltage drop on forward current increased. On the other hand gold diffusion which has a profound effect in decreasing the lifetime by an order of magnitude or more also decreases the radiative efficiency to a similar extent.

The long-wavelength ($\lambda > 1.6\mu$) component of radiation which has been observed with forward-current operation of planar-diffused diodes

is unexpected. The data (Tables I and II) show that it is usually less than 1%, if it is measurable, for $\underline{p}^+$-$\underline{n}$ diodes. However, for $\underline{n}^+$-$\underline{p}$ diodes it is often substantial, particularly for high-resistivity base material and for deeply-diffused diodes. The same trend is barely evident for diodes made on $\underline{n}$-type material.

The dependence of the long-wavelength radiation on the magnitude of the forward current was investigated for an XLD-3(100dp 1.5) diode. It was found that as the forward current increased into the region of rising voltage the proportion of long-wavelength radiation increased (Table III). With 11 V voltage drop at 9.22 A the electric field within the silicon was not less than 10^3 V/cm. In this high a field the holes would become heated to a high temperature. However, it is not clear why a greater effect should appear when holes travel from a $\underline{p}$ to an $\underline{n}^+$ region than vice versa.

The possibility of a thermal effect must be considered. The change of temperature of the region of the silicon die under the junction has been calculated on an adiabatic basis (Table III). It can bee seen that there is no direct correlation between the temperature rise and the increase in long-wavelength radiation. The temperature rise given for the 1.2 msec pulse is too high because the pulse length is probably an order of magnitude longer than the thermal time constant for the device. The radiation from a thermal source would increase exponentially with reciprocal temperature which is a far faster rate than that observed.

Table III. The variation of long-wavelength radiation with the forward current through an XLD-3(100dp 1.5) diode and the calculated adiabatic temperature increase.

Current (A)	Voltage Drop (V)	Pulse Length (sec)	Adiabatic ΔT deg K	Percent Radiation $\lambda > 1.6\mu$	Percent Radiation $\lambda > 1.95\mu$
1.1	5.7	$1.2 \cdot 10^{-3}$	900 [a]	4.0	
3.08	9	$1.6 \cdot 10^{-5}$	53		21
9.22	11	$1.6 \cdot 10^{-5}$	193		35

[a] The actual ΔT would be an order of magnitude less in this case because the pulse is much longer than the thermal time constant of the device.

The experiments of Davies and Storm[20] in regard to recombination radiation from silicon under strong-field conditions showed that considerable spectral broadening of the forward-current radiation resulted at high fields at lower as well as at higher energies. However, their data did not extend to photon energies less than 1 eV. The broadening at higher energies for a sample immersed in liquid nitrogen was explained on the basis of the change in lattice temperature from joule heating. The radiation was shown to be produced by decay of excitons which are at the temperature of the lattice. However, the broadening toward longer wavelengths remained unexplained.

[20] L. W. Davies and A. R. Storm, Phys. Rev. 121, 381 (1961).

Although the observation that $\underline{n}^+$-$\underline{p}$ diodes show more long-wavelength radiation than p^+-$\underline{n}$ diodes implies that hot electrons are the origin of it, the possibility that intraband transitions of hot holes could explain it can not be ignored. Moreover, the possibility of thermal origin of this radiation must still be considered; even though the evidence from one experiment is against it, all possibilities have not been excluded.

At forward-current densities less than about 10^3 A cm^{-2} the XLD-3(100d) diodes show a nearly linear variation of light with current and a slowly rising voltage drop (Fig. 5). The voltage variation observed would be expected from the familiar diode equation

$$I = I_s \left[\exp (eV/kT) - 1 \right]$$

where $V = V_a - V_d$ with $\underline{V_a}$ the applied voltage and $V_d = (kT/e) \ln(n_n p_p / n_i^2)$; $\underline{n_n}$ and $\underline{p_p}$ are the electron and hole concentrations in the $\underline{n}$- and $\underline{p}$-type regions, respectively, $\underline{n_i}$ is the number density of charge carriers for intrinsic semiconductor material, and $\underline{I_s}$ is the saturation current.

At higher current densities the voltage begins to rise as $\underline{i}^{\underline{n}}$ where $1/2 < \underline{n} < 2/3$. Also the light output begins to rise less rapidly than I (Fig. 5). Jonscher[21] has shown in detail that at high current densities the motion of

---

[21] A. K. Jonscher, J. Electron. and Control 5, 1(1958); ibid. 5, 226 (1958).

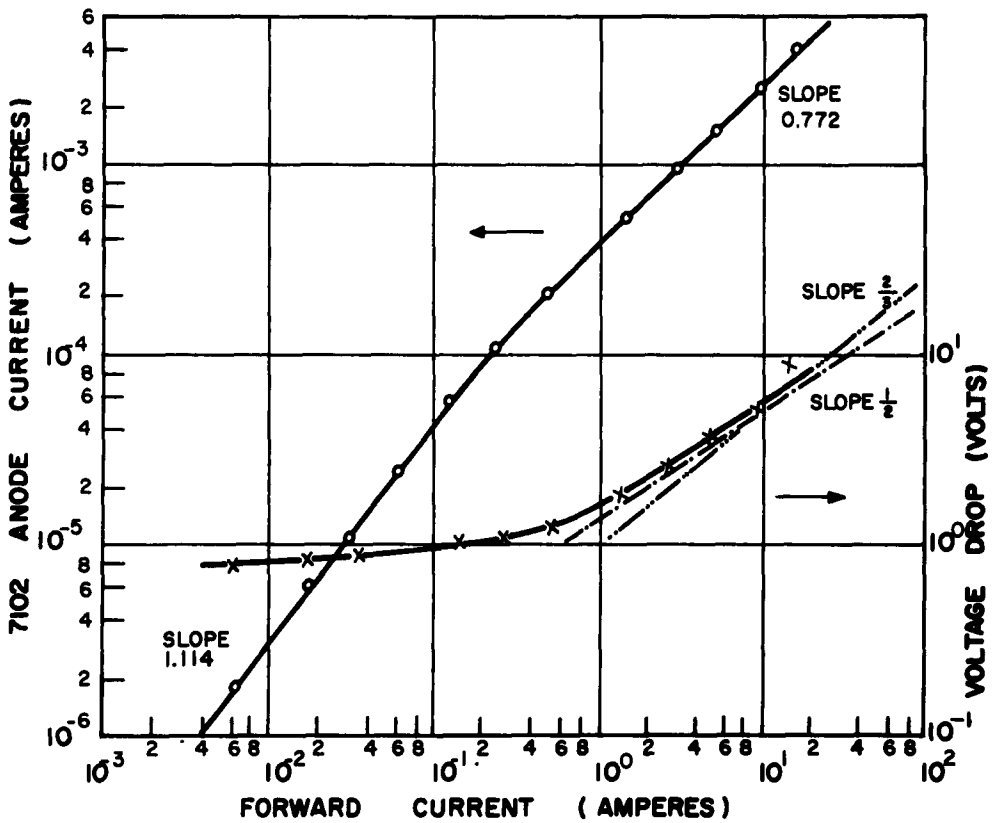

Fig. 5. Light output and voltage drop vs forward current through an XLD-3(100dn .068) diode. The light output is given in terms of the 7102 photomultiplier anode current.

the charge carrier is no longer diffusive, that the majority- and minority-carrier densities become comparable in magnitude and that the effect of the electric field on both species of carrier must be considered. Jonscher's result was that $V \propto I^{\frac{1}{2}}$ when the mobility is taken to be constant. However, Dacey[22] has taken into account the fact that at high fields the mobility μ of the charge carriers in a crystal such as silicon[23] or germanium[24] varies as the inverse root of the electric field E, i.e. $\mu \propto E^{-\frac{1}{2}}$. Consequently at high fields we now find $V \propto I^{2/3}$. Therefore, as can be seen (Fig. 5) the V-I curve begins to approach a slope of 2/3 at the highest currents.

The specific reason for the slower than linear rate of rise of light with current in the region of high current density is not clear. However, in the case of the p^+-n diode (Fig. 5), for example, the light initially is produced by recombination of holes in the n region as they diffuse in from the p^+ region. As the electric field increases the holes begin to travel under the action of the electric field in straighter paths at higher speeds which carry them farther into the interior. Furthermore, Haynes et al.[6] have found that the recombination cross-section σ for charge

---

[22] G. C. Dacey, Phys. Rev. 90, 759 (1953).

[23] E. J. Ryder, Phys. Rev. 90, 766 (1953).

[24] E. J. Ryder and W. Shockley, Phys. Rev. 139 (1951).

carrier varies approximately as the inverse square of the charge-carrier speed. Accordingly, we would expect that electron-hole recombinations would occur less frequently as the current density increases. Increasing attenuation by the increasing thickness of silicon which the radiation traverses does not seem to be important because the intensity of the radiation from the surface of the silicon wafer opposite that in which the junction was diffused was found to be little different than from the front face in one case.

The Variation of Junction Gradient with Diffusion Time

In order to verify that the junction depth was varying properly with diffusion, $\underline{C}$-vs-$\underline{V}$ data were obtained for three diodes made on 0.068-ohm-cm, $\underline{n}$-type silicon without and with diffusion for 1/4 and 1 hour at 1200°C (Fig. 6). The diode with "predeposited" boron has a junction too abrupt to show $\underline{C} \propto \underline{V}^{-1/3}$ and too gradual for the $\underline{C} \propto \underline{V}^{-\frac{1}{2}}$ characteristic of an abrupt junction. However, the unit which had been diffused for 1/4 hour at 1200°C showed a $\underline{C}$ varying closely as $\underline{V}^{-1/3}$ and a gradient $\underline{a} = 6.93 \cdot 10^{21}$ cm^{-4}. The unit which had been diffused for 1 hour at 1200°C yielded $\underline{a} = 3.50 \cdot 10^{21}$ cm^{-4} which is just half that for the previous diode, as it should be, because the junction depth varies as the square root of the diffusion time. The gradient for a junction diffused into a material with a uniform impurity concentration is inversely proportional to the depth of the junction.

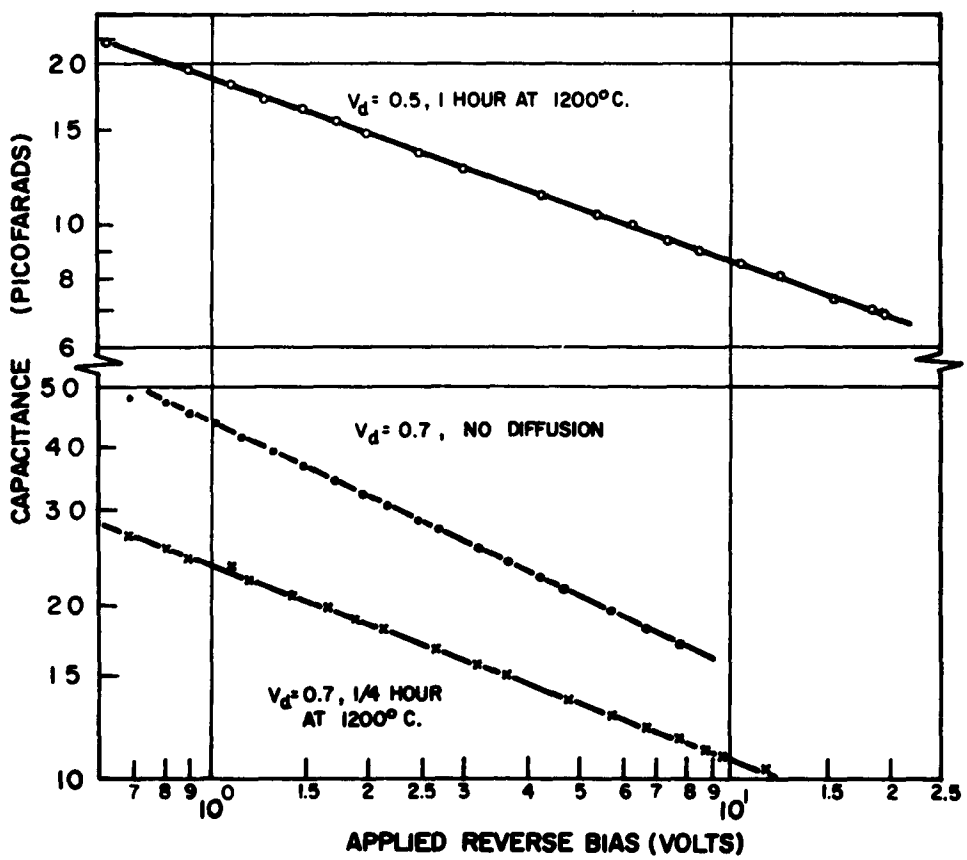

Fig. 6. Junction capacitance vs applied reverse-bias voltage for XLD-3(100dn .068) diodes with an undiffused (predeposited) junction and with junctions diffused for 1/4 and 1 hour at 1200° C.

Recombination Radiation at Liquid-Nitrogen Temperature

The effect of temperature on the total quantity of recombination radiation in silicon has been observed to be a rise or a fall with a decrease of temperature depending on the origin of the radiation. Haynes et al.[6] observed a decrease with temperature of the recombination radiation which resulted either from illumination of the silicon with a strong light or from a forward current passed through a p-n junction. The spectrum changed substantially with temperature. Davies and Storm[20] observed an increase about in inverse proportion to temperature for the reverse-current radiation in a silicon p-n junction without much change in the spectrum. Pokrovsky and Svistunova[15] have investigated the radiative recombination of electrons at un-ionized indium atoms in silicon. Their results were obtained with silicon doped n-type with antimony to an electron concentration of $5.8 \cdot 10^{15}$ to $2.7 \cdot 10^{16}$ cm^{-3} and also containing $1.4 \cdot 10^{15}$ to $6 \cdot 10^{16}$ cm^{-3} indium atoms. The lifetime of the electrons deduced from photoconductivity-decay measurements was about 10 microsec at 300° K and increased as exp (E_i/kT) where $E_i = 0.16$ eV proved to be equal to the ionization energy of indium. At liquid-nitrogen temperature the lifetime was more than 0.1 sec.

When an n-type silicon sample which was doped with indium as described above was illuminated with radiation in the absorption edge to produce electron-hole pairs, it was found that recombination radiation was emitted at 0.97 eV with the silicon at liquid-nitrogen temperature. The intensity of the radiation emitted corresponded to one photon for

each recombination of an electron at a neutral-indium center. Therefore, the use of indium as a recombination center would appear to offer a means whereby efficient production of radiation might be accomplished with silicon.

Accordingly, silicon which contained $5 \cdot 10^{15}$ to $2 \cdot 10^{16}$ cm^{-3} indium atoms and which was doped with phosphorous to make it 0.25-ohm-cm, n-type was obtained. In addition, silicon doped to 0.46, 6.5 and 52-ohm-cm p-type was also obtained. With these materials diodes of the p^+-n and n^+-p type could be made for experiments on the production of radiation in indium-doped silicon. Pokrovsky and Svistunova[15] found that the capture cross-section of ionized indium for holes is about $2 \cdot 10^{-16}$ cm^2 while the capture cross-section of neutral indium for electrons is $4 \cdot 10^{-22}$ cm^2 at 80°K. Therefore, in order to have a good probability for electron capture, it is necessary that there be almost no ionized indium present. Otherwise all available holes would be quickly taken up by the ionized indium and few would remain to recombine with electrons at neutral indium.

Several experiments were made in a search for the radiation which would arise out of the efficient process of electron recombination with the emission of photons at indium in silicon at liquid-nitrogen temperature. Before cooling the diodes to liquid-nitrogen temperature, an evaluation was made at room temperature (Table IV). It was found that on the whole indium-doped diodes were about equivalent to the previously observed diodes doped with boron or phosphorous to a similar resistivity with the exception that all p-type, indium-doped diodes showed an unreasonably large amount of long-wavelength radiation on

Table IV. The radiative efficiency of indium-doped, silicon diodes.

Resistivity of Base Material (ohm-cm)	Diffusion (°C, h)	Breakdown Voltage (volts)	Forward Current			Reverse Current	
			Photons[a] / Electron	Percent Radiation $\lambda > 1.6\mu$	Radiative Lifetime (nanosec)	Photons[a] / Electron	Percent Radiation $\lambda > 1.6\mu$
52 p	-	180	1.7 to $8.8 \cdot 10^{-6}$[b]	2.8 to 7.3[b]	600	-	-
6.5 p	-	70	$3.9 \cdot 10^{-6}$	6.6	<325>	-	-
6.5 p	1200, $\frac{1}{4}$	soft	$2.9 \cdot 10^{-6}$	9.1	290	-	-
6.5 p	1200, 1	180					
0.46 p	-	17	$7.4 \cdot 10^{-7}$	11	-	$2.6 \cdot 10^{-6}$	81
0.46 p	1200, $\frac{1}{4}$	20	$9.6 \cdot 10^{-7}$	4.1	95	$2.4 \cdot 10^{-6}$	58
0.46 p	1200, 1	24	$1.4 \cdot 10^{-6}$	3.5	145	$2.2 \cdot 10^{-6}$	60
0.25n(P+In)[c]	-	18		0.6[d]	260	$3.4 \cdot 10^{-6}$	51

[a] These data apply to the photon flux in air on one side (2π steradians) of the diode; to obtain the total internal flux over 4π steradians multiply by 65 to allow for internal reflections and for emission over all angles.

[b] The smaller numbers apply to a 1 A, 0.5 microsec pulse and to a 0.4 A, 1.2 msec pulse; the higher figures apply to a 1 A, 1.2 msec pulse which may entail heating.

[c] The 0.25-ohm-cm, n-type material is doped with about 10^{16} cm^{-3} indium atoms; enough phosphorous was added to obtain the n-type resistivity given.

forward current and a somewhat larger than usual amount on reverse current; the diode made on the indium-doped silicon, which contained phosphorous to make it n-type, behaved about like phosphorous-doped material of similar resistivity.

Upon cooling the indium-doped diodes to liquid-nitrogen temperature, it was found that the diodes made on 0.46-ohm-cm, indium-doped silicon behaved in a manner comparable to those made on 0.25-ohm-cm, p-type silicon. Both showed about one-half as much forward-current radiation at 77°K as at 300°K and both showed an increase in reverse-current radiation (Table V). However, the 0.25-ohm-cm, n-type, indium-doped silicon behaved very differently (Table V).

Table V. The effect of liquid-nitrogen temperature (77°K) on the radiative efficiency of silicon p-n junctions, mostly indium doped, in ratios relative to 300°K data (all junctions were undiffused).

Resistivity of Base Material (ohm-cm)	Breakdown Voltage	Forward Current		Reverse Current
		Photons/Electron	Radiative Lifetime	Photons/Electron
6.5p(In)		1.1 to 1.0 peak 0.5 to 0.8 plateau	0.1	-
0.46p(In)	1.6	0.5	-	2.3
0.25n(P,In)	0.8	0.3	0.3	1.25
0.25p(B)	1.6	0.5	0.5	3.9

The forward-current radiation from this diode decreased by about four times when cooled to 77°K while the reverse-current radiation hardly changed; the radiative time constant decreased to about one third of its 300°K value.

The 6.5-ohm-cm, p-type, indium-doped silicon diodes behaved entirely differently. At liquid-nitrogen temperature the resistivity of the base material became high and no current would flow until a voltage of 15 to 30 volts was applied for a fraction of a microsecond. When the diode was operated at currents of about 1 A, the initial voltage rose as high as 137 V for a very brief time and then settled down at 25 to 65 V. The initial voltage spike had a width of less than 40 nanosec at half height which may have been determined by the time constants of the equipment. The current rose to a constant value in about 80 nanosec. At the end of the voltage spike and the current rise, a peak in light output of about 50-nanosec width appeared which had started to rise at the peak of the voltage pulse. The peak in light output was comparable to the level of light at room temperature. It was followed by a plateau of light level about half that observed at room temperature. The radiative time constants for the plateau were less than 20 nanosec and were limited by the apparatus.

It may be that in the high-resistivity, indium-doped silicon at low temperature there are many electron traps that must be filled before conduction may proceed after the manner that will be described later in connection with double-injection diodes.

The reduction of the radiative efficiency for forward current can be readily understood on the basis of the experiments of Haynes et al.[6] As they observed at low temperature, only radiative processes associated with the emission of phonons may occur because no phonons are present that may be absorbed in the emission process. At room temperature the conservation of momentum required for the diagonal transition in E-k space may be met both by the absorption and the emission of phonons which are present in reasonable supply. Therefore, radiation may take place in twice as many ways and the intensity should be roughly twice as large which is in accord with the observations.

The increase in the efficiency observed for reverse-current radiation ranged from 2.3 to 3.9 times when the diodes were cooled to 77°K (about 1/4 room temperature) (Table V). A similar increase was reported by Davies and Storm.[20] An explanation for this entirely different temperature dependence lies partly in the voltage drop which may increase considerably (Table V) as a consequence of the reduced charge-carrier gradient at low temperature which increases the voltage drop. The electron-hole temperature in the microplasmas is probably much higher than that of the lattice so that little effect would be expected when the lattice is cooled. No change was seen in the spectral distribution of the radiation by Davies and Storm.[20]

The question remaining is the failure to observe the radiation reported to occur with high efficiency by Pokrovsky and Svistunova.[15] One possibility that was explored was that the lifetime of an electron

trapped by a neutral indium atom is so long that the current would have to flow for a long period before a sufficient number of electrons were trapped in a metastable state to yield an adequate rate of radiative decay for observation. The dependence of the light output on pulse length was examined for pulses from 0.2 to 15 000 microsec long and no dependence of light intensity was observed. Possibly still longer pulses would be necessary. However, the rapid radiative build-up and decay rates observed indicate that all charge carriers are being disposed of quickly; none seem to be being lost to a slower radiative-decay process.

Of course, Pokrovsky and Svistunova[15] were obtaining charge carriers of both sign by photoionization. Possibly substantial concentrations of charge carriers of both signs are needed in the process which they observed. Possibly again intrinsic radiation is necessary to the process of decay which they observed.

The work of Haynes[9] which demonstrated the existence of electronic complexes in silicon at 25°K is of considerable interest in regard to the behavior of indium and other impurities. These complexes consist of an ionized donor and two electrons which bind a hole to the donor or of an ionized acceptor and two holes which bind an electron to the acceptor. The radiative process then consists of recombination of an immobilized electron and hole with the emission of a photon with and without the emission of a transverse-optical phonon. The mechanism whereby such a complex is created was not given by Haynes.[9]

Radiation from such complexes was produced by Haynes by illumination of a doped, silicon crystal with an intense light. The radiation consisted of two lines of width less than $5 \cdot 10^{-4}$ eV separated by 0.058 eV, the energy of a transverse-optical phonon.

Double-Injection Diodes

The theory of Bess[8] has shown that under the condition of a large concentration of both types of charge carrier that the conduction-band-to-valence-band (interband), radiative-recombination processes would become dominant. According to his theory the interband radiative-transition rate would vary as the product of the carrier concentration, i.e. as $\underline{n}_e \underline{n}_p$ in which the two concentrations would be nearly equal, whereas the radiationless transitions would vary as the 3/2 power of carrier concentration. Therefore, a device in which the carrier concentrations are made much higher than those which can be recombined non-radiatively at impurities or defects at the concentration in which these are present should show increased efficiency for the generation of radiation. The negative resistance which has been reported in theory[25] and experiment[26 - 28] for double-injection diodes is an effect which is

---

[25] M. Lampert, Phys. Rev. 125, 126 (1962).

[26] N. Holonyak, Jr., S. W. Ing., Jr., R. C. Thomas, and S. F. Bevacqua, Phys. Rev. Letters 8, 426 (1962).

[27] N. Holonyak, Jr., Proc. Inst. Radio Engrs. 50, 2421 (1962).

[28] L. I. van Ruyven and W. H. Th. Adriaens. Phys. Letters 3, 109 (1962).

closely allied with the effects of high concentration on radiation which were just described. In this case all traps and charged scattering centers become saturated and cease to impede the flow of current so that the resistance of the device drops. Under these conditions interband, radiative recombination should increase in importance.

For this reason experiments were undertaken in which the efficiency of the production of radiation by double-injection diodes was studied. However, the speed of charge-carrier motion in the high electric fields needed to overcome space-charge effects in these diodes may be responsible for the failure of these diodes to exhibit the enhanced efficiency sought except implicitly as will be described. The recombination cross-section σ has been observed by Haynes et al.[6] to vary as $v^{-2} = |\vec{v}_e - \vec{v}_h|^{-2}$ so that the recombination rate R which is given by $R = n_e n_n \sigma v$ varies as v^{-1}; $\vec{v}_e$ and $\vec{v}_h$ are the electron and hole velocities.

The experiments with double-injection diodes yielded valuable results about the recombination of electrons and holes in heavily-doped p- and n-type regions, respectively. Also, with these diodes it was possible to show that linear variation of light with current is observed when a charge carrier recombines in a heavily doped region of the opposite majority-carrier type; and that square-law variation of light with current takes place when the diode consists of overlapping, heavily-doped regions so that the charge-carrier product is about equal to the square of the individual concentrations. These points have not before been explicitly exhibited.

Fabrication of Double-Injection Diodes

Double-injection diodes have been made by diffusing boron and phosphorous into adjacent regions of a ca. 300-ohm-cm, n-type silicon wafer 6-mils thick. These devices are identified as XLD followed by a series number and a number in parentheses which gives the dimensions of the gap between the p- and n-type areas in tenths of a mil, e.g., XLD-1(40x200) has a gap 4-mils wide by 20-mils long (Fig. 7). Phosphorous was predeposited at 1200°C for 20 min. and boron at 1150°C for 30 min. When the double-injection diode was subsequently subjected to diffusion, the temperature in °C and time in hours follow the dimensions outside the parentheses, e.g., XLD-1(40x200) 1280, 4 was diffused for 4 hours at 1280°C.

Forward-Current Performance

Units of this kind have been examined for the dependence of light output on current, for the time constant for the response of light to current flow, and for V-I characteristics. The variables in these investigations have been junction width, depth of diffusion, and gold content. The results for forward-current operation will be discussed here and for reverse-current operation in the next section.

Regional Variation of Light Intensity

The junction width was found to have little influence on the light-producing characteristics of the XLD diodes in comparison with

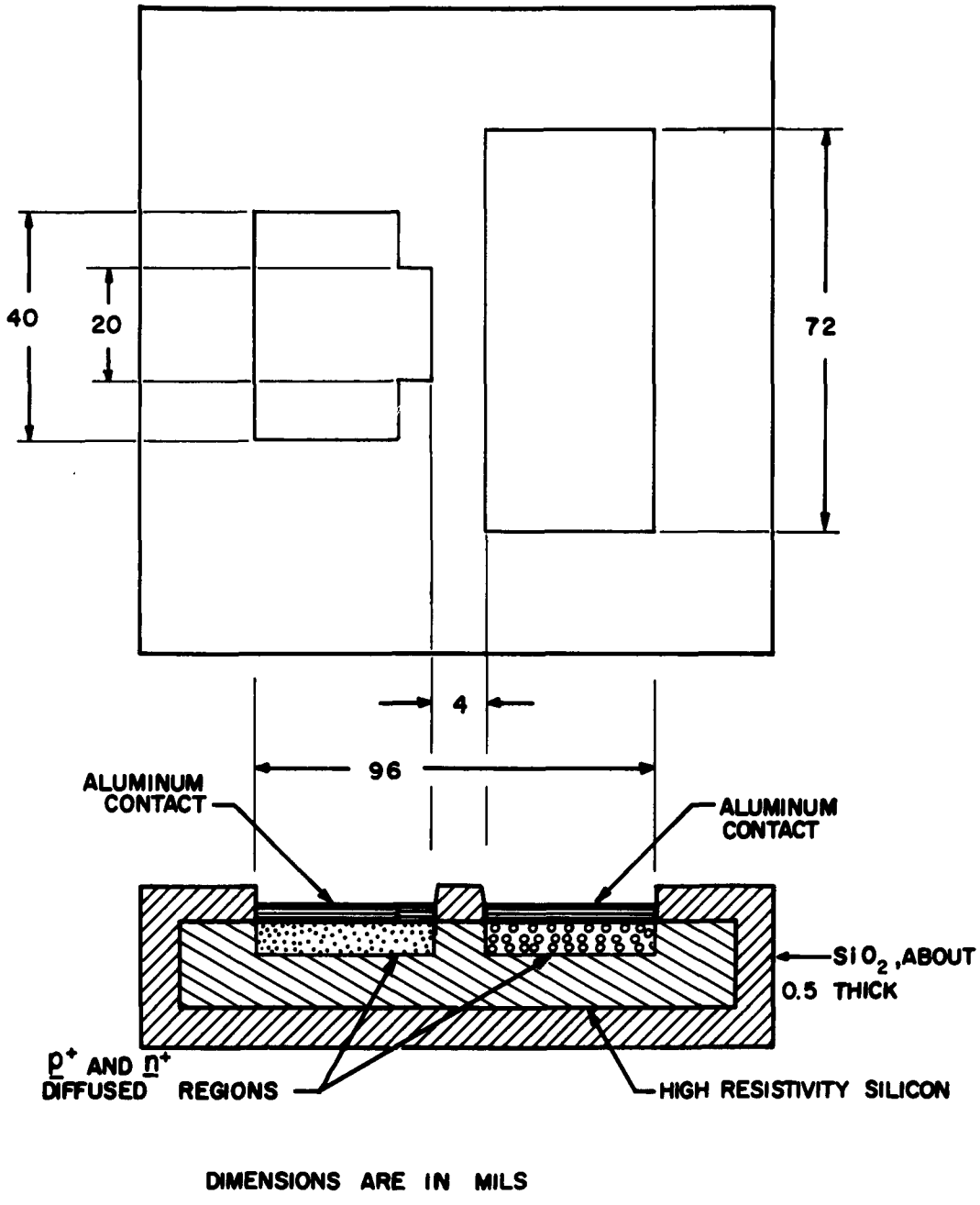

Fig. 7. The dimensions of an XLD-1(40x200) double-injection diode (not to scale).

other properties of the device. However, for the study of light production in a diode operating with forward current the XLD-1(40x200)-type with injection pads separated by 4 mils was very useful. The junction was scanned with a slit which was about 1.3-mils wide and was oriented parallel to the edges of the injection pads. It was found that the light intensity was a maximum at the edge of the $\underline{p}^+$ pad and that the width of the source was less than that of the slit. With the light flux taken as 1 from the edge of the $\underline{p}^+$ pad the flux at the edge of the $\underline{n}^+$ pad was 0.4 and from the high-resistivity $\underline{n}$-type region between the pads the flux was 0.16 per slit width (Fig. 8). The high resistivity region is about 3-slit-widths wide so that the total light from recombination in this region is comparable to that from the $\underline{n}^+$ and $\underline{p}^+$ regions. These measurements were verified by observation with an infrared image converter (Fig. 9).

The ratio of the light from the $\underline{p}^+$ and $\underline{n}^+$ regions was 2.5 to 1. This ratio is very nearly equal to the drift-mobility ratio $\mu_{\underline{n}}/\mu_{\underline{p}}$ of 2.6 for $\underline{n}$-type silicon with an impurity density less than 10^{14} cm^{-3}.[29] The mobility ratio begins to decrease at high field so that at the fields employed, which were ca. $9 \cdot 10^3$ V cm^{-1}, the applicable mobility ratio would be somewhat less than the drift-mobility ratio. Therefore, it appears that for the radiation detected by a 7102 photomultiplier ($\lambda < 1.2$ microns) the probability of radiative recombination of electrons in the $\underline{p}^+$ region is nearly equal to that for holes in the $\underline{n}^+$ region because the ratio of the electron to hole current is equal to the $\mu_{\underline{n}}/\mu_{\underline{p}}$ ratio. This result

---

[29] A. B. Phillips, Transistor Engineering (McGraw-Hill Book Co., New York, 1962), p. 69.

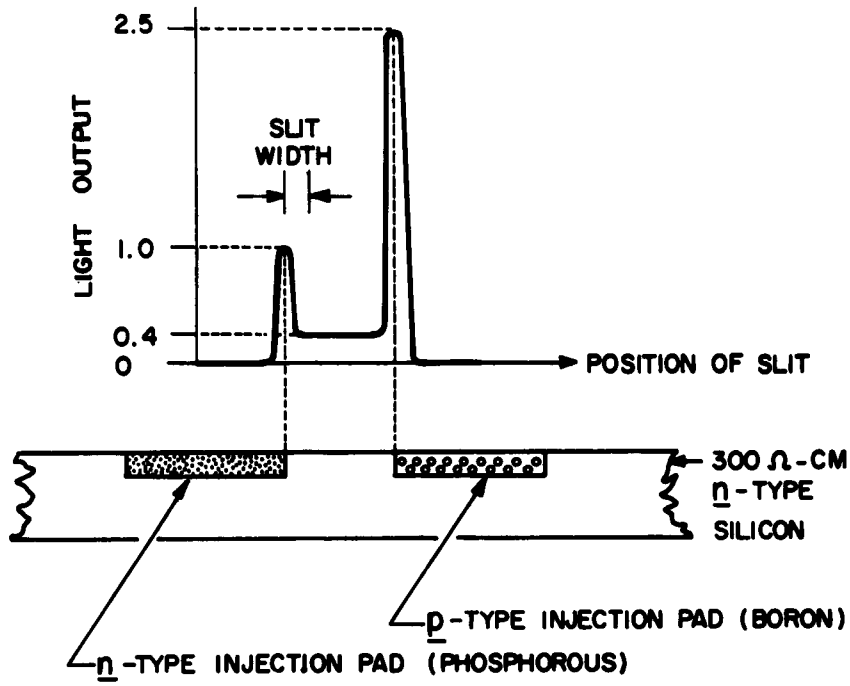

Fig. 8. Light output as a function of slit position across an XLD-1(40x200) operated at 9.2 A forward current.

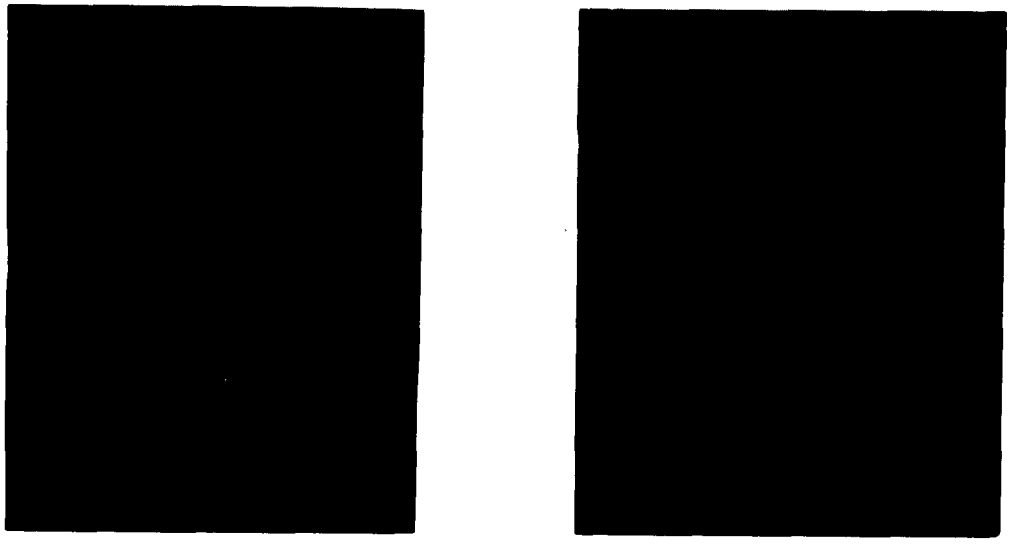

(a) (b)

Fig. 9. The radiation from an XLD-1(40x200) 1280, 4 double-injection diode as seen through an infrared image converter with an overall magnification of about 85X. (a) The diode with external illumination. (b) Radiation at the edges of the $\underline{p}^+$ region (lower left) and $\underline{n}^+$ region (upper right). Pulses 2.5 microsec long at 1 A for a total of $8 \cdot 10^5$ pulses or a total duration of 2 sec were used.

is somewhat unexpected and may be a coincidence; no reason is known for the necessity of this equivalence of radiative recombination probabilities in the two different regions.

The expectation that radiative-recombination probability in the high-resistivity region would be higher than in the $\underline{n}^+$ and $\underline{p}^+$ regions is indicated by the observation that the total radiation from this region is comparable to that from the boundaries of the $\underline{n}^+$ and $\underline{p}^+$ regions. The drift velocity of holes and electrons in the high-resistivity region would be of the order of $5 \cdot 10^6$ cm sec^{-1} at $9 \cdot 10^3$ V cm^{-1} so that the number density of electrons and holes there would be of the order of 10^{15} cm^{-3} for a current of 10 A. The recombination rate in this region would be proportional to $\underline{n} \cdot \underline{p} \approx 10^{30}$ cm^{-6}. In the $\underline{n}^+$ and $\underline{p}^+$ regions for which the charge-carrier number density is of the order of 10^{19} cm^{-3}, or more, the products $\underline{n} \cdot p_{\underline{p}}$ and $\underline{p} \cdot n_{\underline{n}}$ would be of the order of $10^{15} \cdot 10^{19} = 10^{34}$ cm^{-6}. Therefore, the $\underline{n} \cdot \underline{p}$ product is 10^4 times greater in the $\underline{n}^+$ and $\underline{p}^+$ regions. With a photon flux from the intervening region comparable to that in the $\underline{n}^+$ and $\underline{p}^+$ regions we would estimate that the probability of radiative recombination in the high-resistivity region is of the order of 10^4 times greater than in the heavily doped regions. The light observed from the high-resistivity region may have partially arrived by internal reflection and/or scattering in the oxide so that this result is not quantitative.

The inability to obtain a higher efficiency of light production in the double-injection diodes used stems from the high electric field needed to obtain a substantial current in the presence of space-charge effects which causes the relative velocity between electrons and holes to be large.

By constructing a device in which the injection is accomplished from a highly-doped region with a thin, diffused region of the opposite conductivity type between each injector and with a drift region of high-resistivity material, it might be possible to reduce the electric field in the drift region so that the recombination product could be greatly increased there.

The Effect of Diffusion Depth on Light Production

In an effort to reduce the detrimental effect of radiationless, surface recombination on the production of light, diodes of the XLD-2(4x200)-type were diffused for 2 and 4 hours at 1280°C after predeposition of boron and phosphorous. In this way the injection pads were extended more deeply into the volume of the high-resistivity material on which they were placed. With deeper injection pads the current between them would flow farther away from the surface thus reducing the proportion of recombinations there. However, the light generated by recombination of the charge carriers farther below the surface would have to pass through more material to escape and thus would suffer additional absorption. Therefore, there would be an optimum depth of diffusion.

As it turned out, the light output per unit of forward current varied as 1:4:2 for units predeposited, diffused for 2 hours, and for 4 hours, respectively. It appears from these data that the optimum depth may correspond to a diffusion time of less than 2 hours at 1280°C. It is estimated that 2 hours at 1280°C may increase the depth of current flow to 4 times that with no diffusion and that 4 hours will increase the depth by an additional factor of 2.

The V-I Characteristics of Double-Injection Diodes

According to the theory of Lampert[24] a double-injection diode should exhibit a negative resistance in its V-I characteristic. This prediction has been confirmed by the experiments reported.[26 - 28] Experiments were, therefore, carried out with the XLD-1(40x200) diode. A current ramp was generated from a high-current pulse from a pulse-forming network discharged by a 4C35A hydrogen thyratron. It was found that with a current ramp rising at a rate of $4 \cdot 10^6$ A sec^{-1} a negative slope appeared in the voltage curves at about 0.8 A. However, with a ramp rising at a rate of $2.5 \cdot 10^5$ A sec^{-1} the negative-resistance region disappeared. Therefore, it was concluded that the negative resistance observed was a dynamic effect.

A pinch effect has been reported in InSb by Glicksman and Powlus[30] and by Chynoweth and Murray[31] and has been considered theoretically by Glicksman.[32] The simple criterion of Chynoweth and Murray for the occurrence of a pinch is $i_{co} = 2kT/ev$ where i_{co} is the critical current, T is the temperature of the electron-hole plasma, and v is the speed of the charge carriers in the electric field under which they move through the pinch. In our experiments the field was about $3 \cdot 10^3$ V cm^{-1} for which v is about $6 \cdot 10^6$ cm sec^{-1}, if the increased electron-lattice interaction

---

[30] M. Glicksman and R. A. Powlus, Phys. Rev. 121, 1659 (1961).

[31] A. G. Chynoweth and A. A. Murray, Phys. Rev. 123, 515 (1961).

[32] M. Glicksman, Phys. Rev. 124, 1655 (1961).

at high fields is ignored. Then we find $i_{co} \approx 0.9$ A for high-resistivity silicon under the assumption that the plasma temperature is about equal to room temperature. Therefore, the assumption that the dynamic, negative resistance arises from the pinch effect appears to be substantiated.

In order to determine whether a static, negative resistance could be achieved, an XLD-1 (40x200) diode was diffused with gold for one-half hour at 1010° C to thoroughly saturate it at about 10^{16} gold atoms per cm^3, as was done by Holonyak et al.[26,27] In this way the resistivity of silicon is greatly increased because the impurity levels of gold fall about midway between the valence and conduction bands.

When measurements were made on the gold-saturated, double-injection diode, a negative resistance showed clearly in the V-I characteristic (Fig. 10). For this measurement the current ramp rose at a rate of $2.9 \cdot 10^3$ A sec^{-1} and decayed more slowly. The negative-resistance region started at a current of about 27 mA and voltage of about 25 volts.

There is no doubt that the double-injection diodes can be made to operate as intended. However, even in 300-ohm-cm silicon at currents as high as 4 A all traps have not yet been saturated so that maximum benefit of this mode of operation may not have been achieved. The introduction of gold at a number density about 10^2 times higher than that of the impurity in the initial material allows the negative-resistance effect to be seen clearly. However, recombination at the gold impurity atoms

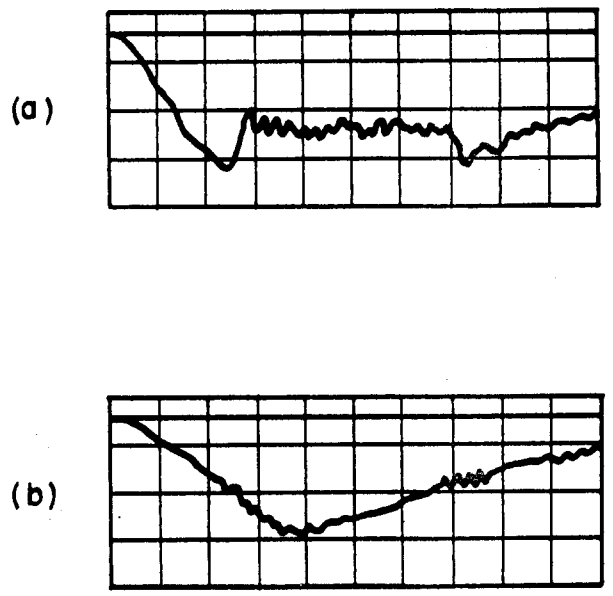

Fig. 10. The negative-resistance in the V-I characteristic of XLD-1(40x200) gold-doped at 1010° C is shown by these facsimiles of oscilloscope traces (a) 10 V/div (vertical), 5 microsec-div (horizontal), (b) 20 mA/div, 5 microsec/div.

reduced the light output to 0.35 of that from a similar diode without gold. This reduction indicates that the recombination of electrons and holes at gold does not yield radiation at wavelengths less than about 1.1 micron, if at any wavelengths.

Light Output as a Function of Current

In general, the light-vs-current characteristics of p-n junctions, such as the XLD-3 diodes or the double-injection diode, are nearly linear at high current densities ($> 10^3$ A cm^{-2}) (Fig. 11). In these cases radiation arises predominantly from recombination in a region doped to a number density higher than that of the injected minority carriers. Therefore, the recombination radiation varies linearly with the number density of the injected carriers.

In a double-injection diode the recombination radiation should vary as the $n \cdot p$ product in the intermediate region and, accordingly, as the square of the current. However, in the double-injection diodes tested thus far this radiation has been small as compared to that from minority-carrier recombination, except at the highest currents, so that current dependence for light in this region has not been measurable in these units.

If, however, the diode is made with the n^+ and p^+ regions superimposed in the predeposition stage, the situation is quite different from that in the previous double-injection diodes or in an XLD-3 diode. Now the injected holes and electrons meet each other in a narrow, highly-doped, approximately-compensated region. The recombination rate

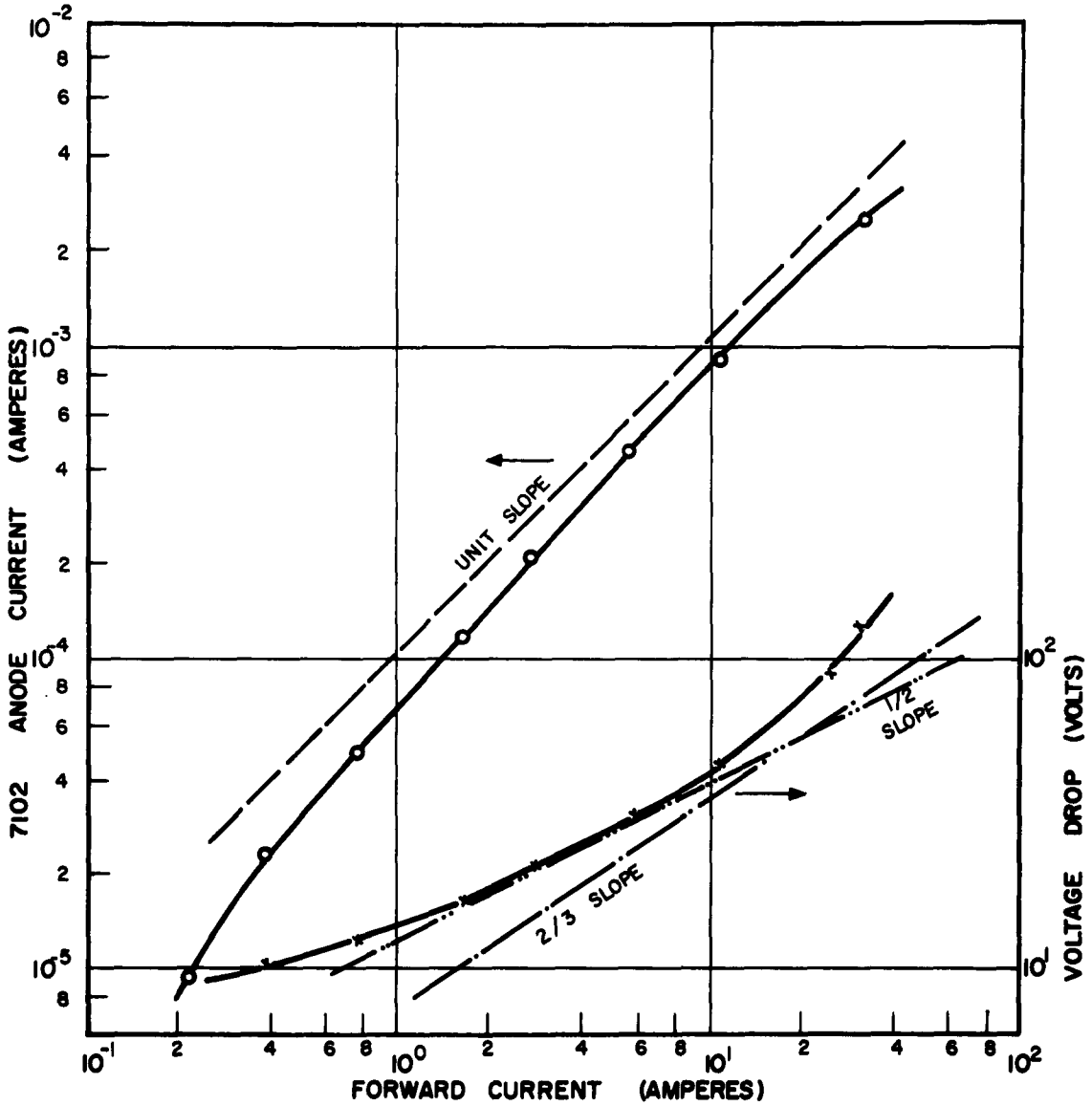

Fig. 11. Light output (in terms of 7102 anode current) and voltage drop vs forward current through XLD-2(4x200)1280, 4.

there would be forced to vary as the $n \cdot p$ product which in turn varies as the square of the current. The light-output-vs-current curve for an XLD-1(-25x200) diode (where the - sign before 25 indicates a 2.5-mil overlap) shows square-law variation at high current levels (Fig. 12).

In all cases the light output varies more rapidly than linearly with current at lower current densities. As has been discussed, Bess[8] has shown that radiationless-recombination processes arising from certain impurities and imperfections will tend to vary more slowly with the carrier-concentration product than the radiative-recombination process so that above some current the latter would dominate.

In the double-injection diodes the geometry leads to very high current densities and high electric fields so that a decrease in mobility as a consequence of the interaction of the charge carriers with the acoustical modes of the lattice becomes important and μ begins to vary as $E^{-\frac{1}{2}}$. Consequently, we find that V varies more nearly as $I^{2/3}$ than as $I^{\frac{1}{2}}$ as high currents are reached, as was discussed earlier in connection with the V-I characteristics of XLD-3(100d) diodes.

Reverse-Current Performance

The same p-n junctions that have been investigated for performance on forward current have, whenever possible, been examined for reverse-current performance. Generally, the breakdown voltage has been high and the efficiency of light production has been inferior to that for the XLD-3(100 d) series of diodes. The geometrical design was not intended for this purpose.

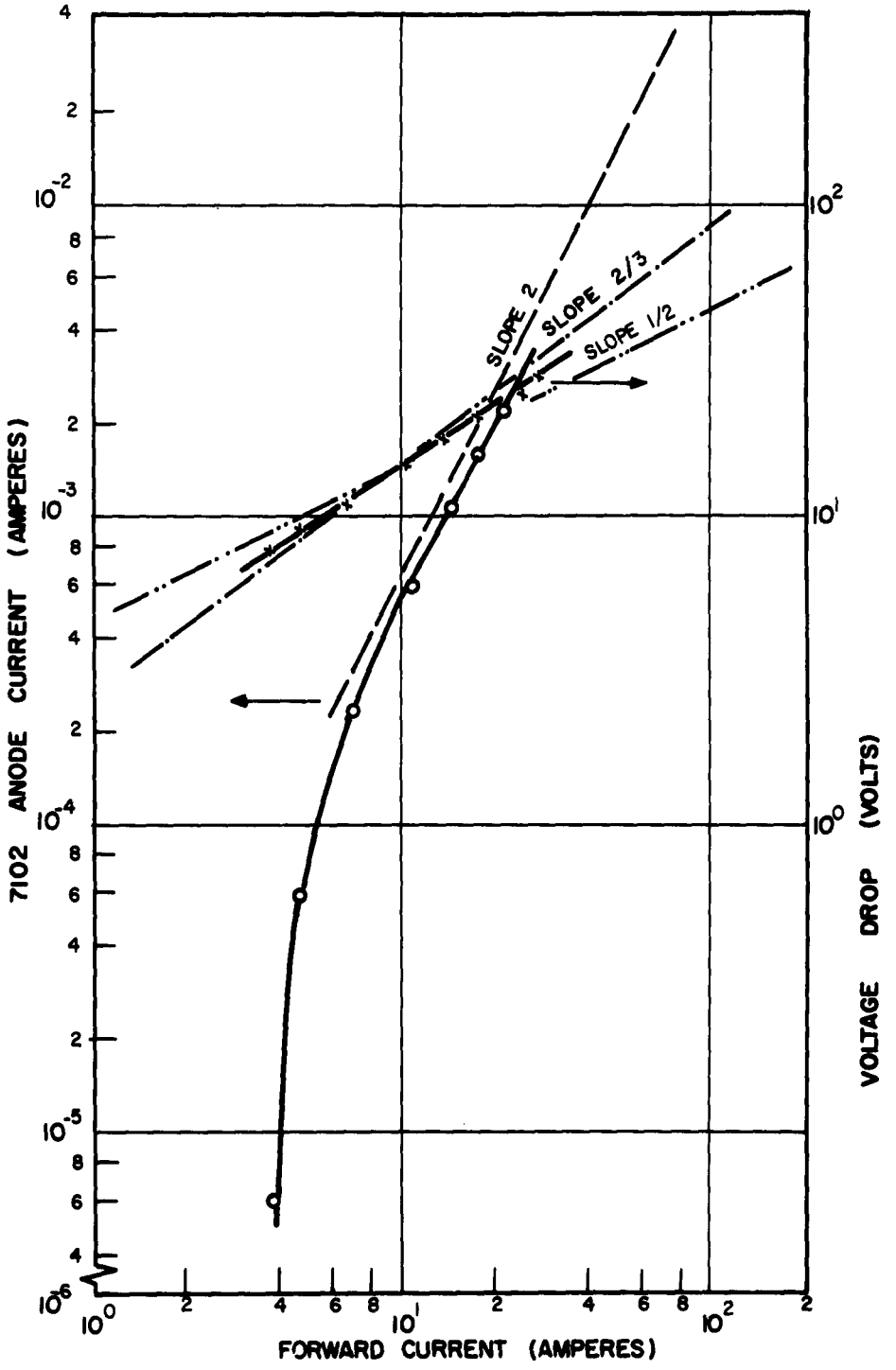

Fig. 12. Light output (in terms of 7102 anode current) and voltage drop vs forward current through XLD-1(-25x200).

Long-Wavelength Radiation

An experiment was carried out with a $\underline{p^+}$-$\underline{n}$-$\underline{p^+}$ diode made in the XLD-2(40x200) linear, planar geometry and made on 300-ohm-cm, $\underline{n}$-type silicon in an effort to associate the production of long-wavelength radiation with hot holes. Holes were injected by pulsing one $\underline{p^+}$-$\underline{n}$ junction and were then accelerated by voltages of up to -67.5 V on the second $\underline{p^+}$ pad with respect to the $\underline{n}$-type region. No effect was noticed on radiation of any wavelength when the potential was applied to the second $\underline{p^+}$ pad; only about 10% of the injected hole current was collected because of the poor geometry of the device. Higher voltages could not be used because the $\underline{p^+}$-$\underline{n}$ junction would breakdown. The results, though negative in regard to the production of long-wavelength radiation by holes, are not highly significant because of the small electric fields which would be applied to the holes.

3. OPTICAL COUPLING OF CIRCUIT ELEMENTS

The radiation emitted by a small source in a medium in sheet form with a high index of refraction is largely entrapped by internal reflection if the external medium is one with a lower refractive index, such as air. For example, it will be shown that in the case of silicon, for which the refractive index $\underline{n} = 3.56$ at 1 micron, only about 2.7% of the radiation emitted over 2π steradians (a hemisphere) would be available outside a plane surface in air. The problem of optical coupling without the aid of optical design is a serious one when semiconductor light sources and receivers are to be used.

Although placing the source and receiver in close proximity would eliminate inverse-square losses, the intrusion of unwanted electrical coupling requires a device separation which amounts to several times its dimension transverse to the direction of coupling.

A light pipe is an elementary device which utilizes to advantage the internal reflection which was the origin of the problem. A transparent rod of a material with a high index of refraction will be shown to be an efficient means of carrying radiation from one point to another point centimeters to many meters away. Similarly, with suitable entrance geometry, a laminar-light-guide system may be used.

However, at all times it is necessary that there be no substantial discontinuity in the index of refraction in the system so that light pipes

must have an index approaching that of the semiconductor materials. Furthermore, any joint between the two must be made with a cement having a comparably high refractive index.

The theory of a light pipe and its application to the evaluation of some materials as light pipes for use with silicon will be presented. A selection of low-melting, high-index glasses which have been tried will be discussed. The application of laminar optics to the problem will be examined. Experimental results with light-coupled transducers and light-operated devices, such as a flip-flop, will be presented.

The Theory of Light-Pipe Performance

A rod of transparent material which has a higher index of refraction than that of the medium in which it is immersed will transmit a substantial amount of light from one point to another by multiple internal reflection. As long as the diameter of the rod corresponds to a large number of wavelengths of the radiation being carried, the classical-optical concepts apply and the device will here be called a light pipe. When the diameter of the rod is of the order of a few wavelengths it will behave much as a waveguide. In this case the device will be called an optical fiber. Despite the distinction between light pipes and optical fibers many of the considerations are similar so that much that has been written about optical fibers may be studied to advantage.[33]

---

[33] N. S. Kapany in J. Strong, Concepts of Classical Optics (W. H. Freeman and Co., San Francisco, 1958), Appendix N, pp. 553-579.

The use of light pipes for optical interconnection of a light source and receiver made of semiconductor material is important for several reasons: (1) Without a light pipe most of the light generated in a material with a high refractive index is trapped within it by internal reflection, and that which escapes is subject to a refractive loss (less than 3% per hemisphere would escape from silicon into air). (2) If the receiver is removed from the source by, say, ten times its diameter to reduce the electrical coupling, it subtends a solid angle corresponding to

$$2\pi\,(1 - \cos \tan^{-1} 1/20) \simeq 2\pi/800 \text{ sterad.}$$

so that only about 1/8% of the light available over a hemisphere would reach the receiver even if it were immersed in the same medium as the source. (3) In order to transfer light any appreciable distance, or to convey it around obstacles, there is no alternative to a light pipe.

Accordingly, it is important to consider the problem of transferring light from the medium in which it is generated into the medium of the receiver when both media have a high refractive index as is characteristic of a semiconducting material such as silicon.

The first case to consider is that in which the light source is in a material from which the light emerges into a medium of lower refractive index through a plane surface. In the second case a right-cylindrical light pipe of equal or lower refractive index is placed on the exit surface. The inverse case, i.e. the reentry of light from a light pipe into the medium of higher refractive index, which involves only reflection losses,

is implicit in the treatment. Therefore, the light transfer by a light pipe, neglecting losses within the pipe, is readily obtained from the same calculations. For simplicity, the treatment will be confined to meridional rays, though it is known from the work of Potter et al.[34, 35] that skew rays make an appreciable contribution.

First we consider the case in which light originates in a medium i and enters a medium r through a plane interface, where n_i and n_r are the respective refractive indices of these media (Fig. 13). The light flux in r may be expressed in terms of the angle r and the ratio $\rho = n_i/n_r$ for the two polarizations $\parallel$ and $\perp$ coresponding to the cases in which the electric vector is parallel and perpendicular to the plane of incidence. The fluxes $\phi_\parallel$ and $\phi_\perp$ are given by

$$\phi_\parallel(r) = \int_o^{\pi/2} \frac{4\,\rho^{-1} \sin r \cos^2 r}{\left[\sqrt{1-(\rho^{-1}\sin r)^2} + \rho \cos r\right]^2}\, dr,$$

$$\phi_\perp(r) = \int_o^{\pi/2} \frac{4\,\rho^{-1} \sin r \cos^2 r}{\left[\rho\sqrt{1-(\rho^{-1}\sin r)^2} + \cos r\right]^2}\, dr,$$

---

[34] R. J. Potter, J. Opt. Soc. Am. 51, 1079 (1961).

[35] R. J. Potter, E. Donath, and R. Tynan, J. Opt. Soc. Am. 53, 256 (1963).

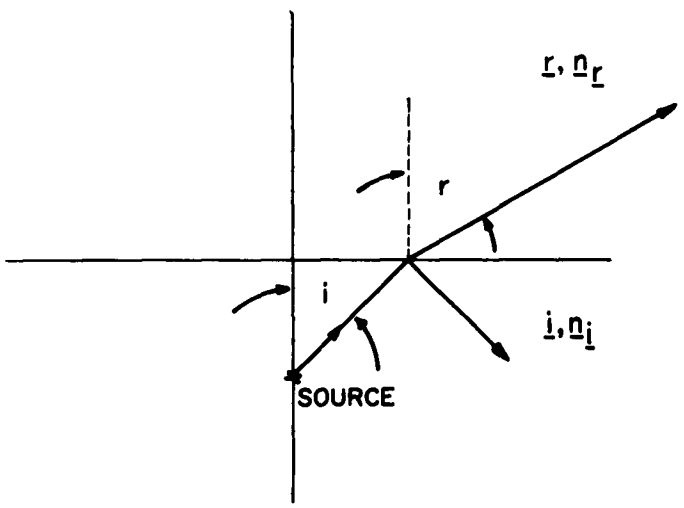

Fig. 13. The path of light from a source in medium $\underline{i}$ of refractive index $\underline{n}_{\underline{i}}$ to a point in medium $\underline{r}$ with refractive index $\underline{n}_{\underline{r}}$.

where the integration is carried over 2π steradians (a hemisphere) in medium $\underline{r}$ and a unit flux of each polarization has been assumed over 2π steradians in medium $\underline{i}$.

In the next case a light pipe of refractive index $\underline{n}_{\underline{r}}$ is placed over the light source in medium $\underline{i}$ of refractive index $\underline{n}_{\underline{i}} \geq \underline{n}_{\underline{r}}$ and the whole assembly is immersed in a medium with unit refractive index (Fig. 14). Then only that radiation which is incident on the surface of the pipe at an angle greater than the critical angle $\sin^{-1} 1/n_r$ will be transmitted by the pipe. The fraction of the light flux emitted by the source in $\underline{i}$ over 2π steradians in the two polarizations is given by the equations

$$\phi_{\parallel}(r)_{pipe} = \int_0^{r_c} \frac{4\rho^{-1} \sin r \cos^2 r}{[\sqrt{1-(\rho^{-1} \sin r)^2} + \rho \cos r]^2} \, dr,$$

$$\phi_{\perp}(r)_{pipe} = \int_0^{r_c} \frac{4\rho^{-1} \sin r \cos^2 r}{[\rho\sqrt{1-(\rho^{-1} \sin r)^2} + \cos r]^2} \, dr,$$

where $r_c = \pi/2 - \sin^{-1} 1/n_r$ and $\rho = n_i/n_r$ as before.

The equations for $\phi_{\parallel}(r)$ and $\phi_{\perp}(r)$ given above have been graphically integrated for the indices of refraction of several materials which have been used to construct light pipes. Plots (Figs. 15 to 18) of the integrands for glasses with refractive indices of 1.84 and 2.47 show

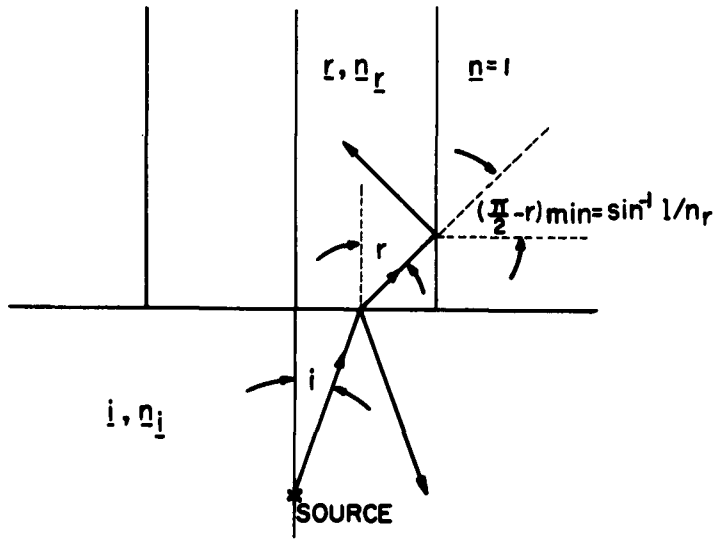

Fig. 14. The path of light from a source in medium $\underline{i}$ with a refractive index $\underline{n}_{\underline{i}}$ into a light pipe of index $\underline{n}_{\underline{r}}$ immersed in a medium of unit index.

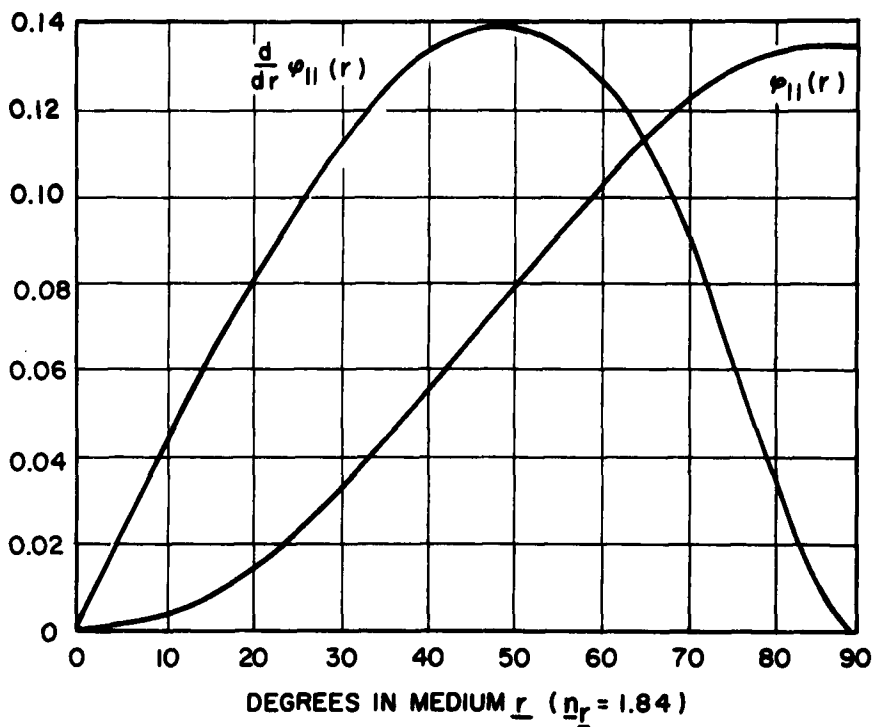

Fig. 15. A plot of d $\phi_{\parallel}(r)/dr$ and $\phi_{\parallel}(r)$ vs r for a medium r with n_r = 1.84 and a source medium i with n_i = 3.56.

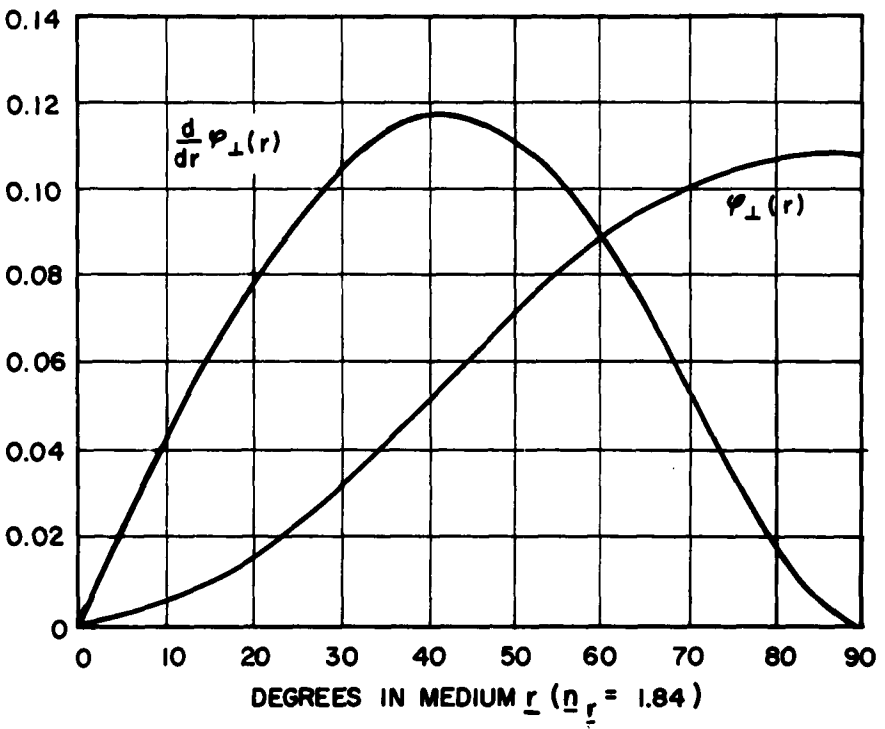

Fig. 16. A plot of $d\phi_\perp(r)/dr$ and $\phi_\perp(r)$ vs r for a medium r with $n_r = 1.84$ and a source medium i with $n_i = 3.56$.

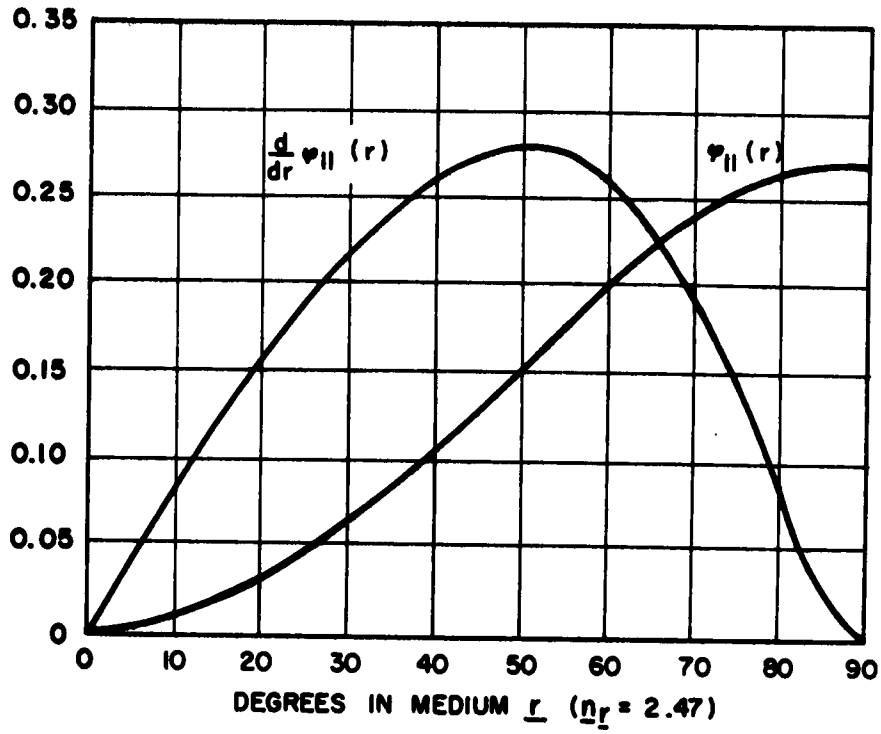

Fig. 17. A plot of $d\phi_{\parallel}(r)/dr$ and $\phi_{\parallel}(r)$ vs r for a medium r with $n_r = 2.47$ and a source medium i with $n_i = 3.56$.

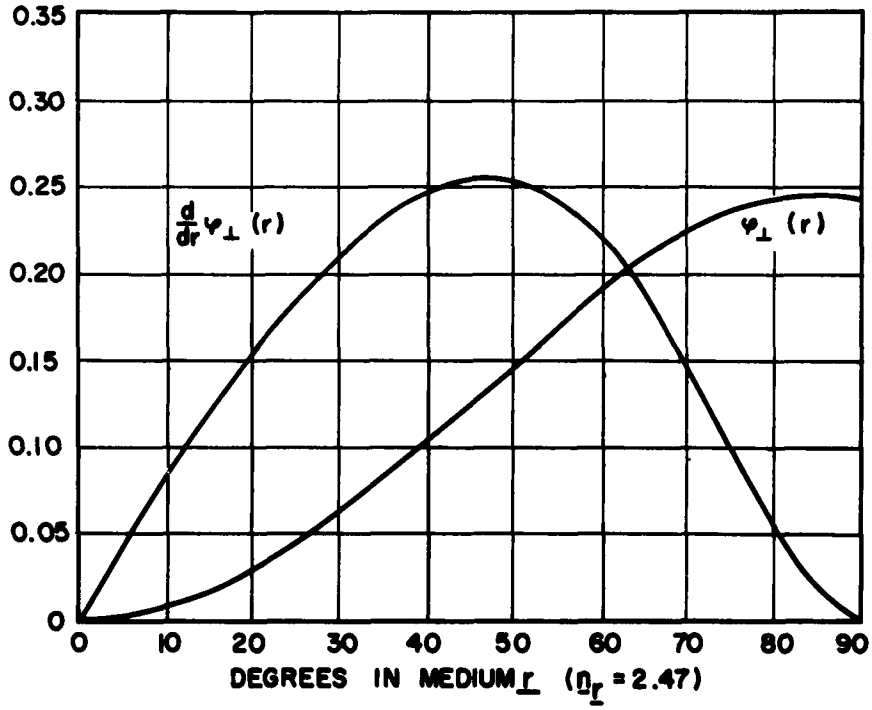

Fig. 18. A plot of $d\phi_\perp(r)/dr$ and $\phi_\perp(r)$ vs r for a medium r with $n_r = 2.47$ and a source medium i with $n_i = 3.56$.

that the principal portion of the emergent radiation can only be obtained if it is collected over most of the hemisphere, i.e. only if the light pipe has a refractive index approaching that of the medium containing the source.

When all of the calculated data are gathered together (Table VI) and plotted (Fig. 19) it is clearly evident that careful attention must be given to the selection of a light-pipe material with a suitably high refractive index. Furthermore, fractions are tabulated not only for the entrance of light into the light pipe but also for the exit of it so that to calculate the overall transfer of light from source to receiver the fractions must be multiplied.* Thus a light pipe of Pyrex with $\underline{n} = 1.47$ would transfer $0.0386 \cdot 0.869 = 0.0335$ of the light available over 2π steradians while one of arsenic trisulfide with $\underline{n} = 2.47$ would transfer $0.216 \cdot 0.953 = 0.206$ of that available. Although a factor of $0.206/0.0335 = 6.15$ has been gained, much of the light is still being lost in the overall transfer.*

The case in which a layer of material of refractive index $\underline{n}_1$ intermediate between the refractive index $\underline{n}_i$ of the medium of the light source and of an external medium of refractive index $\underline{n}_2$ has also been examined. Here the intermediate layer is considered to be thick compared to the wavelength of the radiation so that multiple reflections in this layer are treated incoherently (Fig. 20). The fractions of the

---

*These calculations were incorrect in Interim Engineering Report No. 2.

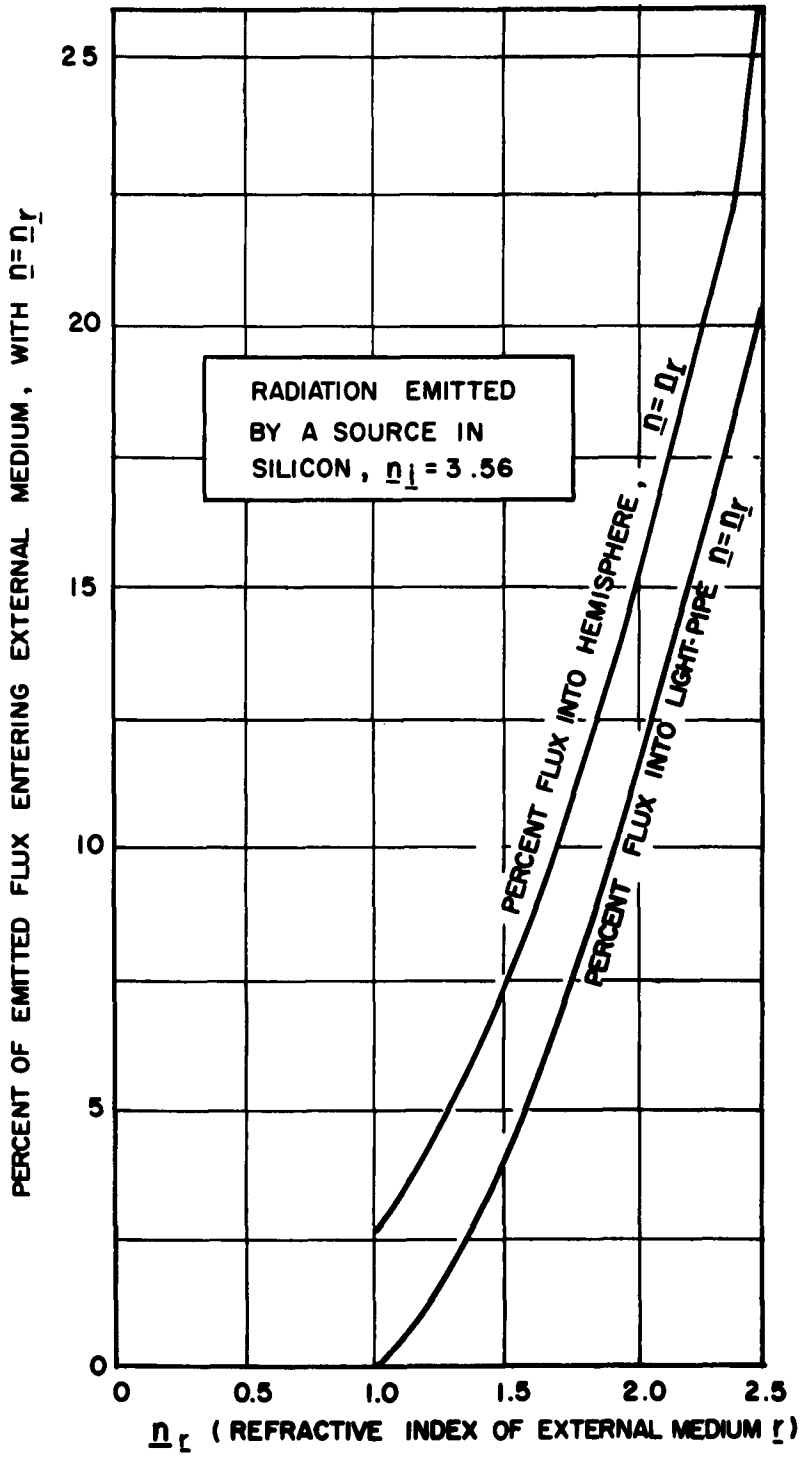

Fig. 19. The light flux available from a source in a medium with $n_i = 3.56$ over 2 π steradians in medium r with index n_r and from a light pipe of index n_r immersed in a medium of unit refractive index as a function of n_r.

Table VI. The percentage of radiation which escapes from a source in silicon ($\underline{n}$ = 3.56) through a plane surface into an external medium and into a light pipe with several values of refractive index and the percent of light in the light pipe that re-enters a silicon receiver (values are given for the materials cited at 1 micron).

External Index of Refraction	Plane Surface			Entering Light Pipe			Re-entering Silicon
	$\phi_\perp/2$	$\phi_\parallel/2$	$(\phi_\perp + \phi_\parallel)/2$	$\phi_\perp/2$	$\phi_\parallel/2$	$(\phi_\perp + \phi_\parallel)/2$	
1	1.05	1.66	2.71	0	0	0	-
1.47[a]	2.96	4.05	7.01	1.82	2.04	3.86	86.9
1.84[b]	5.39	6.77	12.2	4.18	4.74	8.92	89.2
2.2	8.70	10.18	18.9	7.29	8.04	15.3	93.0
2.47[c]	12.0	13.4	25.4	10.4	11.2	21.6	95.3
3.56[d]	100	100	100	35.9	35.9	71.8	100

[a] Pyrex, Corning Glass Co.

[b] IR 20, Bausch and Lomb

[c] As_2S_3, American Optical Co.

[d] Si

available over a hemisphere in medium $\underline{i}$ are given for both polarizations by the equations

$$\phi_\parallel(r_2) = \int_0^{\pi/2} \frac{(1 - r_{i1}^\parallel)(1 - r_{12}^\parallel)}{1 - r_{i1}^\parallel r_{12}^\parallel} \frac{\rho_{i2}^{-2} \sin r_2 \cos r_2}{\sqrt{1 - (\rho_{i2}^{-1} \sin r_2)^2}} dr_2,$$

$$\phi_\perp(r_2) = \int_0^{\pi/2} \frac{(1 - r_{i1}^\perp)(1 - r_{12}^\perp)}{1 - r_{i1}^\perp r_{12}^\perp} \frac{\rho_{i2}^{-2} \sin r_2 \cos r_2}{\sqrt{1 - (\rho_{i2}^{-1} \sin r_2)^2}} dr_2,$$

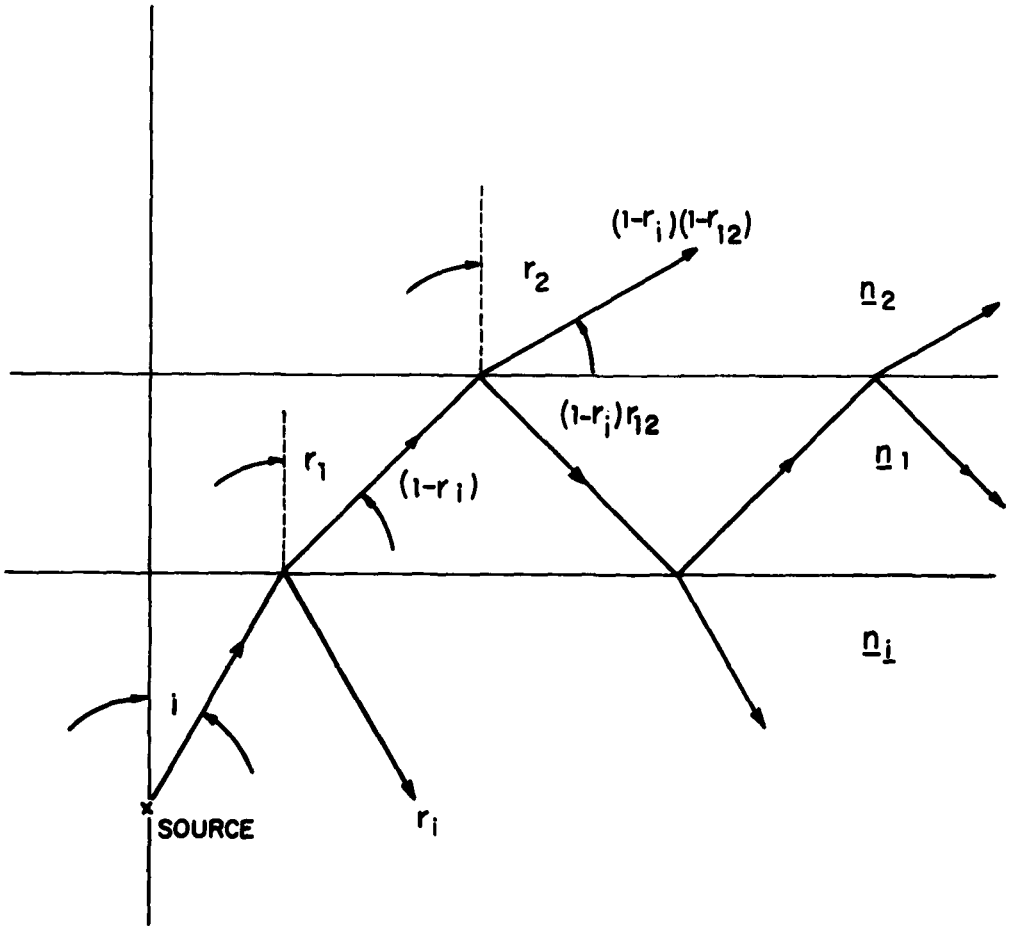

Fig. 20. The exit of light from a medium $\underline{i}$ of index $\underline{n}_{\underline{i}}$ through a thick layer of index $\underline{n}_1$ into an external medium 2 of index $\underline{n}_2$ where $\underline{n}_{\underline{i}} > \underline{n}_1 > \underline{n}_2$. The multiple reflection in 1 are incoherent.

where

$$r_{i1}^{\parallel} = \left[\frac{\rho_{i1}\{1 - (\rho_{12}^{-1} \sin r_2)^2\}^{\frac{1}{2}} - \{1 - (\rho_{i2}^{-1} \sin r_2)^2\}^{\frac{1}{2}}}{\rho_{i1}\{1 - (\rho_{12}^{-1} \sin r_2)^2\}^{\frac{1}{2}} + \{1 - (\rho_{i2}^{-1} \sin r_2)^2\}^{\frac{1}{2}}} \right]^2 ,$$

$$r_{12}^{\parallel} = \left[\frac{\{1 - (\rho_{12}^{-1} \sin r_2)^2\}^{\frac{1}{2}} - \rho_{12} \cos r_2}{\{1 - (\rho_{12}^{-1} \sin r_2)^2\}^{\frac{1}{2}} + \rho_{12} \cos r_2} \right]^2 ,$$

and

$$r_{i1}^{\perp} = \left[\frac{\{1 - (\rho_{12}^{-1} \sin r_2)^2\}^{\frac{1}{2}} - \rho_{i1}\{1 - (\rho_{i2}^{-1} \sin r_2)^2\}^{\frac{1}{2}}}{\{1 - (\rho_{12}^{-1} \sin r_2)^2\}^{\frac{1}{2}} + \rho_{i1}\{1 - (\rho_{i2}^{-1} \sin r_2)^2\}^{\frac{1}{2}}} \right]^2 ,$$

$$r_{12}^{\perp} = \left[\frac{\rho_{12}\{1 - (\rho_{12}^{-1} \sin r_2)^2\}^{\frac{1}{2}} - \cos r_2}{\rho_{12}\{1 - (\rho_{12}^{-1} \sin r_2)^2\}^{\frac{1}{2}} + \cos r_2} \right]^2 ,$$

and

$$\rho_{i1} = n_i / n_1 ,$$

$$\rho_{i2} = n_i / n_2 ,$$

$$\rho_{12} = n_1 / n_2 .$$

Calculations for SiO_2 ($\underline{n}_1 = 1.45$) on Si ($\underline{n}_i = 3.56$) in air ($\underline{n}_2 = 1$) yield 3.08% for the radiation which escapes into a hemisphere in contrast to bare silicon for which 2.71% escapes.

The Techniques and Materials of Optical Transfer

The desirability of semiconductor materials with a high index of refraction for efficient input and output devices places limitations upon materials applicable for light transfer. Among the factors which affect efficient optical transfer, a number are optical-mechanical, such as cement wetting and contact, the effect of beads, fillets, and thickness of cement, rounded edges or surface damage, and contamination in light pipes and such. These factors are generally classed as interface degradation sensitivity. Standard photo-optical terminology[36, 37] is employed in the discussion that follows.

A basic problem in the assembly of opto-electronic devices is the size and optical character of the surface of the light guide. Initially, the silicon dice were cemented onto the pipe, then the whole was supported at the silicon dice. In this construction, no contact of the side optical surface of the guide occurs, but the shipping and handling hazards indicate room for improvement. "Point" and/or "line" contact to support the guide is usable to hold the contact area to a minimum. This construction requires pressure of contact; otherwise vibration will product small digs.

---

[36] MIL-Spec 51-70-2C - The lens, mirror, and prism surface defects and optical glass defects are defined in this specification.

[37] MIL-STD-150A - Military Standard, Photographic Lenses.

It can be shown that for a 0.030-in.-diameter fiber there are roughly 102 reflections per inch for an internal angle of reflection of 20°. Unclad arsenic trisulfide allows effective use of such internal angles (provided that the input index matches the source index). Also, the geometrical-reflected-ray-path length in a straight-side light guide is independent of diameter.[32]

Striae have been recognized visually in the arsenic trisulfide supplied by American Optical. From appearance, the variations in index of refraction are at least 0.003, if not 0.005. Thus path-length differences of a number of wavelength occur. As the striae are not symmetrically located, the effects are random.

The striae which are observed define the geometrical limits of the system as that of one made with "D"-grade optical glass, except for bubbles.[37] Bulk, optical-grade arsenic trisulfide appears capable of "B" and "C"-grade use[38, 39] by selection.

By contrast, Bausch and Lomb IR 20 glass is readily obtainable in "B"-grade homogeneity, stain-test class 2; and light guides, pipes and

---

[38] Servo Corp. of America Data Sheets: Catadioptric Optical System, Part No. 1025032; Servofax, Arsenic Trisulfide Glass, (1961).

[39] American Optical Company Data Sheet: Arsenic Trisulfide Glass: "much of As_2S_3 glass is striated. ---- present production is practically homogeneous."

fibers can be made correspondingly. The lower index of refraction of IR 20 is its chief drawback for use as an unjacketed, single, light guide.

The water solubility of the optical surface of arsenic trisulfide is only 14% worse than that of spectacle crown glass (n_D = 1.5230), but 12% loss of weight per hour in a 2% KOH solution is alarming.[39] We have also observed a rapid surface attack by iodine. Due to the number of reflections the optical guide surfaces cannot be efficient in the presence of thin films even vaguely close to 1/4 wavelength in thickness. Surface contamination is therefore critical for unclad elements[40, 41] to the extent that, for example, spectacle-crown glass is not usable for fibers unless it is covered or jacketed to protect the surface. When arsenic trisulfide is insulated with a plastic of an index n = 1.50, the numerical aperture is 1.96. The use of modified arsenic sulfide as an insulation material for better infrared transmission is limited, as it has the index of 2.41 compared to the core taken at 2.472, which gives a numerical aperture on the same basis of 0.55.

---

[40] W. P. Siegmund, Fiber Optics: Principles, Properties, and Design Considerations, presented before 6th Annual Meeting, AGARD (NATO) Paris, France, July 1962.

[41] N. S. Kapany, Research and Development of Infrared Fiber Optics, Tech. Doc. Rept. ASD-TDR-62-684, Contract No. AF33(616)-8624 (Optics Technology Corporation, October 1962), AD 290 520.

The better homogeneity and surface quality of IR 20 are of interest. Thus if IR 20 is usable for a portion of the system without mismatch or loss from theoretical optical properties, the performance gain is attractive. While Hansell[42] employed internally-reflective, fiber-optical elements for facsimile photo-electric scanning, the system illustrated a conical fiber but did not reveal any conscious historical precedent for numerical-aperture and index-design data. A further search revealed a wealth of references, largely patents,[43, 44] showing similar constructions or applications without index of refraction changes along the optical transmission line. Dicke,[45] for scintillation detection, used a conical "horn" ending to "collimate" the output from an immersed source. He did not show the photo-cathode "wetted" to the large end of the horn, as later practiced. Williamson[46, 47] further detailed the numerical-aperture control as in Dicke, but dealt only with air dielectrics by using mirror surfaces. He established that an internally-reflective cone allows an increase of the flux density within certain limits which is the reverse of Dicke's[45] construction.

---

[42] U. S. Patent 1,751,584, C. W. Hansell, Picture Transmission (1930).

[43] U. S. Patent 1,848,814, R. P. Allen, "Potted" fiber block.

[44] U. S. Patent 2,091,152, J. T. M. Malpica, Oscillogrpah.

[45] U. S. Patent 2,448,963, R. H. Dicke, Detection of High Speed Particles.

[46] U. S. Patent 2,788,708, B. E. Williamson, Apparatus for Collecting From a Field of View.

[47] B. E. Williamson, J. Opt. Soc. Am. 42, 10 (1952).

The labor of formulating a full-skew-ray analysis [34, 35] of the design goals was considered beyond the needs of the program. An analog-study method has been used which inherently limits the geometrical optics to meridian rays. This simplifies the study problem radically. The method is that of fabricating light pipes which are prismatic projections of the meridian sections of axially-symmetrical light pipes. Thus, a square bar is the projection of the meridian section of a cylindrical-light-guide rod. With this type of construction the reflective, refractive, and related surfaces of geometrical-optical design are in one plane. In the plane which truncates the cylinder formed by these surfaces the device operates as an internally-reflective light pipe. [48, 49] Previous experience [50] in optical wiring with such elements indicated that there was experimental expediency in the approach. Such optical constructions are designated as laminar optics, as distinguished from light pipes, fiber optics, and power-surface optics. A laminar, light-pipe horn was investigated (Fig. 21). In the plane of $\underline{d}_1$, $\underline{d}_2$, and $\underline{L}$, this horn is analogous to the tapered fiber operating as [51] $d_1 \sin \theta_1 = d_2 \sin \theta_2$ wherein θ_1 and θ_2 are the entrance and exit angles in the flared plane. In the other

---

[48] U. S. Patent, 3,060,805, C. H. Brumley, Image Forming Element.

[49] U. S. Patent, 3,060,806, R. E. Lewis and R. J. Meltzer, Image Forming Element.

[50] U. S. Patent, 2,868,960, A. V. Appel and R. E. Lewis, Instrument Illuminator (for WADC).

[51] J. W. Hicks, Jr., and P. Kiritsy, Fiber Optics Handbook (Mosaic Fabrications, Inc., Southridge, Massachusetts, 1961).

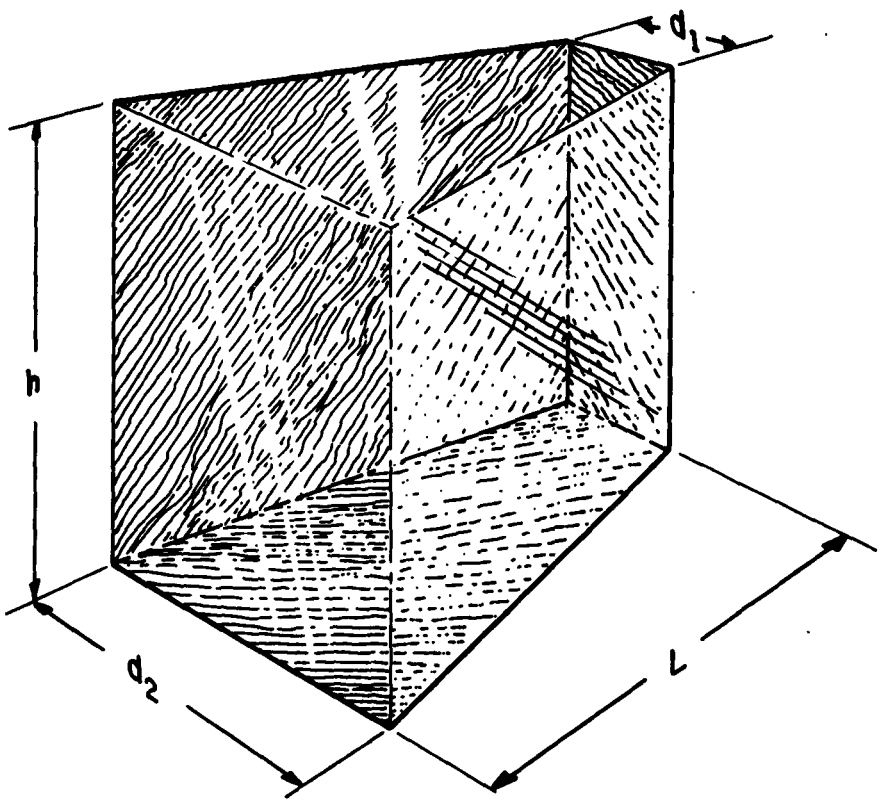

Fig. 21. A laminar-optical light-pipe horn.

plane, containing $\underline{h}$, the optical path obeys the equations of simple fibers (untapered). By definition, numerical aperture is n sin θ. Thus it will be seen that the horn reduces the N. A. of a bundle of rays going from $\underline{d}_1$ to $\underline{d}_2$ as shown. The light entering the small end becomes more collimated as the diameter increases. The reverse path is effective without geometrical loss, if the input horn is identical to the output horn and the two are coupled by a transmission element with parallel faces. This construction avoids exceeding critical angles along the reflection faces and duplicates input and output angles.

Polished Plexiglas study models of index 1.48 - 1.50 were used.[52] In order to transfer the results obtained with the model to a device made of other materials the effect of the change of the index of refraction must be taken into account. The dimensions chosen for test-pieces of type $\underline{A}$ and $\underline{B}$ were $d_1/d_2 = 0.3$, $h = 8d_1$, $L_A = 4d_1$, $L_B = d_1$. In addition, a block $\underline{T}$ of section $\underline{h}$ and $\underline{d}_2$ was used to verify the collimation within the length of the horn (Fig. 22). Plexiglas is particularly useful in this type-study, as it is hazy enough to show visually the ray paths within the material.

The horn and block in the analog were "soldered" by colorless oil with $\underline{n}_D = 1.50$ which makes a fully wetted joint. Axial transmission through the assembly was 0.86 including the input and exit-face reflection losses. The escape condition occurs when the rays enter and leave by the

---

[52] H. Pearson, "Piping Light with Acrylic Materials," Modern Plastics Magazine, August 1946.

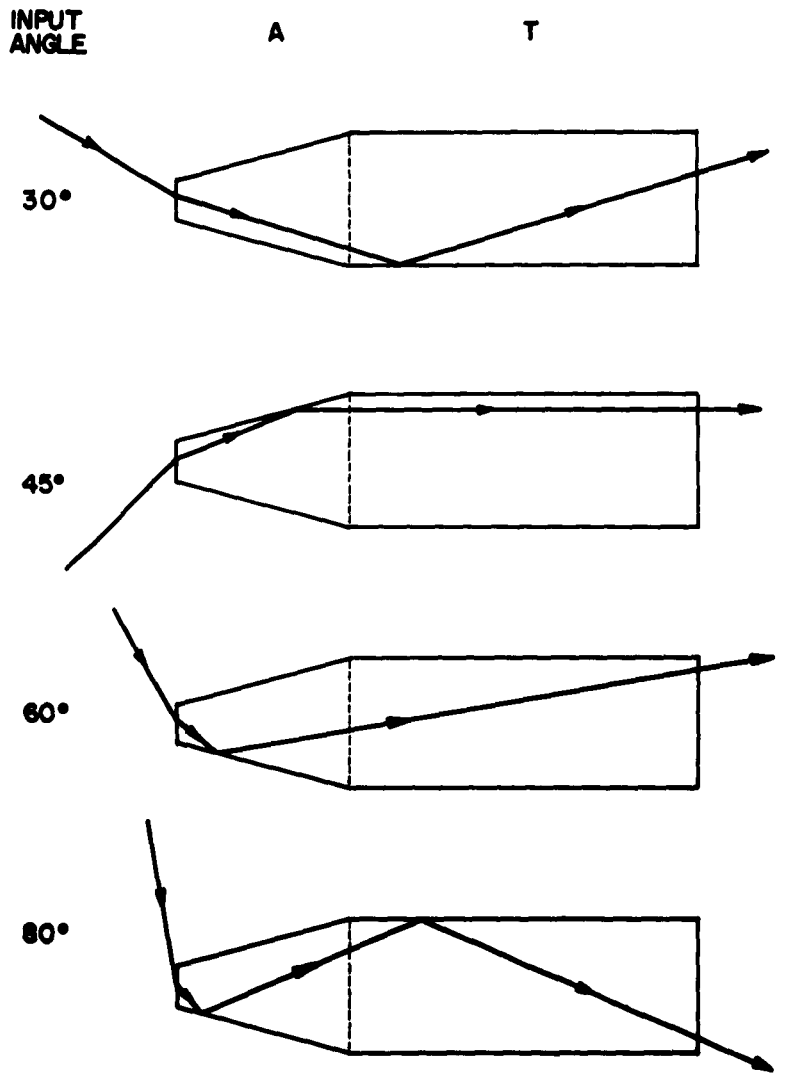

Fig. 22. Collimation within the length of a type-A horn for various angles of incidence at the entrance to the horn.

side, not the end (Fig. 23, 24). A symmetrical system has an A-type horn on each end. The ray trace of a B-type horn ending is different (Fig. 24). Both the A and B-type horns have $d_1/d_2 = 0.3$. Essentially, a 20° taper on an unclad-arsenic trisulfide guide eliminates side escape. With the construction illustrated, the ratio d_1/d_2 determines the collimation in T, and likewise the reflection losses in it. For example, a ray leaving the source at 20° to the face of the die (70° to axis of horn) requires only two reflections to be at 10° to the axis and thereby leaves the horn with no further reflection (immersed). At this angle it could exit to the air. Thus a section of IR 20 glass, or the equivalent, is feasible between arsenic-trisulfide horn ends. This construction retains the value of the higher-index, input-output match with a wider selection of material in between for transmission.

High-Refractive-Index, Inorganic, Cement Glasses

In order to achieve an optically efficient joint between silicon with $n = 3.56$ and As_2S_3 glass with $n = 2.47$ or IR 20 glass with $n = 1.84$, a cement is needed with an index of refraction n_g within the limits given by $3.56 \geq n_g \geq 2.47$ or 1.84. The ideal value for n_g is given by

$$n_g = (n_{Si} n_p)^{\frac{1}{2}}$$

where n_p is the refractive index of the light pipe. In this way the reflection losses at the two interfaces which the cement glass makes with the silicon (or other material) and the light pipe are a minimum.

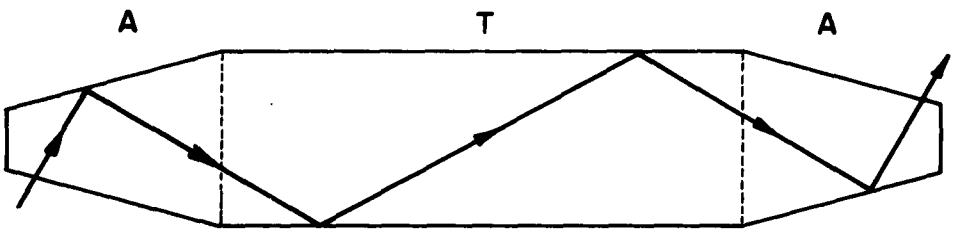

Fig. 23. An illustration of the escape condition for a ray which enters the side of a horn in a symmetrical light-guide system with type-A horns.

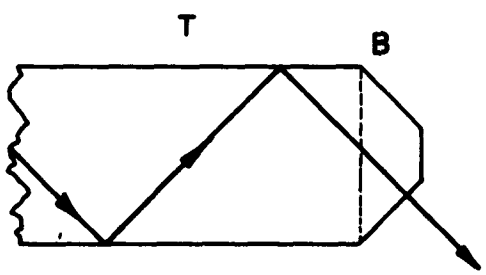

Fig. 24. The escape condition for a ray in a light guide with a type-B horn ending.

The melting point of the cement glass is mainly determined by the requirement that it be less than that of As_2S_3 (300° C[53]), but substantially higher than room temperature. A range of 100° C to 200° C was considered suitable for the melting point of the cement.

An early experiment was made with SnI_4 which melts at 143.5° C, has an index of refraction of 2.11 and has a high electrical resistance. However, SnI_4 sublimes at 180° C[54] so that it proved to be unsatisfactory for the intended purpose. Also the SnI_4 crystallized upon fusion which made the bond mechanically and optically unsuitable.

Subsequent work was devoted entirely to the As-S-Br and As-S-I inorganic glasses which offer a suitable range of melting points within the composition range of the glassy state. The As-S-I system has recently been investigated by Flaschen et al.[55] The As-S-Br system has been reported earlier, but not in such a systematic way, by Meyrowitz.[56]

---

[53] N. A. Lange, Handbook of Chemistry (McGraw-Hill Book Co., New York, 1961), 10th ed.

[54] P. C. L. Thorne and E. R. Roberts, Fritz Ephriam-Inorganic Chemistry (Interscience Publishers, New York, 1954), 6th ed., pp. 345-350.

[55] S. S. Flaschen, A. D. Pearson, and W. R. Northover, J. Appl. Phys. 31, 219 (1960).

[56] R. Meyrowitz, Am. Mineral. 40, 398 (1955).

Fischer and Mason[57] have determined that the composition 33% As, 30% S, and 37% Br (by weight) yields a glass with an index of about 2.4, a softening point of 140° C, a resistivity of 10^{13} ohm cm, and good transparency to 0.55 micron[58] which is adequate for our purposes.

Glasses DG-1 and 2 in the As-S-Br system were prepared (Fig. 25) by heating the elements by flame in a lightly-capped, quartz tube after the manner of Flaschen et al.[55] Glasses DG-7 and 8 in the As-S-I system (Fig. 26) were prepared by heating as before but by starting with fractured As_2S_3 and I; the resulting glasses were more homogeneous. Superior results were obtained by means of a heater for the reaction tube made of an aluminum block with cartridge-type electric heaters. Sample DG-5 (Fig. 26) was prepared this way.

Generally the heating cycles used above were short, the longest being 3 hours for DG-5. Recently reported work[59, 60] shows that

---

[57] A. G. Fischer and A. S. Mason, Investigation of Carrier Injection Electroluminescence, Sci. Rept. No. 3, Contract No. AF 19 (604)-8018 (RCA Laboratories, Princeton, N. J., Nov. 15, 1961), AD 270 128.

[58] ibid., Sci. Rept. No. 2, August 15, 1961, AD 264 433.

[59] C. J. Billian, Investigation of Long Wavelength Infrared Glasses, Int. Engr. Rept. No. 2, Contract No. AF 33(657)-8560 (Servo Corporation of America, July 15 to October 15, 1962), AD 286 989.

[60] Advanced Functional Electronic Block Development, Int. Engr. Rept. No. 2, Contract No. AF 33(657)-9772 (hp Assoc., December 1, 1962, to February 1963).

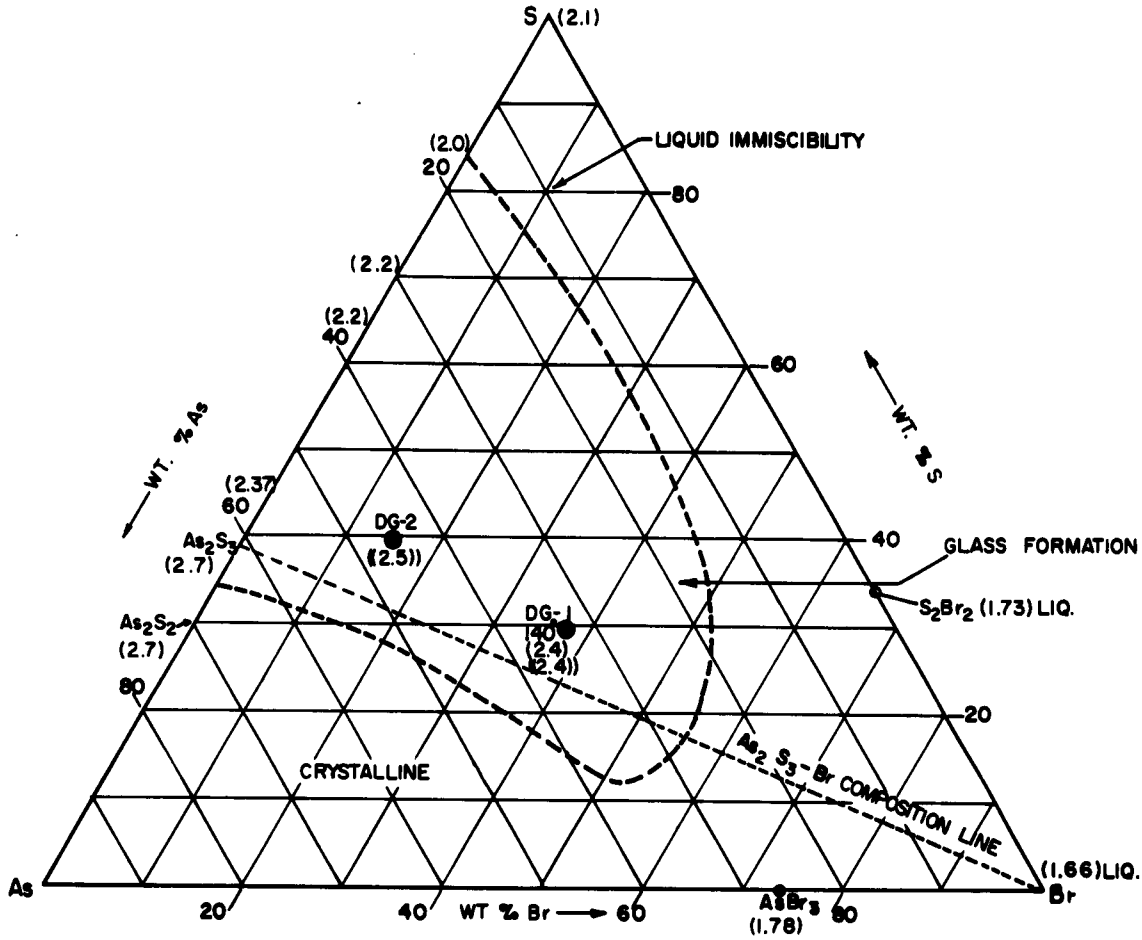

Fig. 25. The phase diagram of the As-S-Br system shows the glass-forming region, softening points in °C, and some indices of refraction. The phase diagram is assumed to be similar to that for As-S-I.[55] The indices of refraction enclosed ( ) are from refs. 53, 56, 57, 60 and those enclosed (( )) are ones measured for material synthesized here.

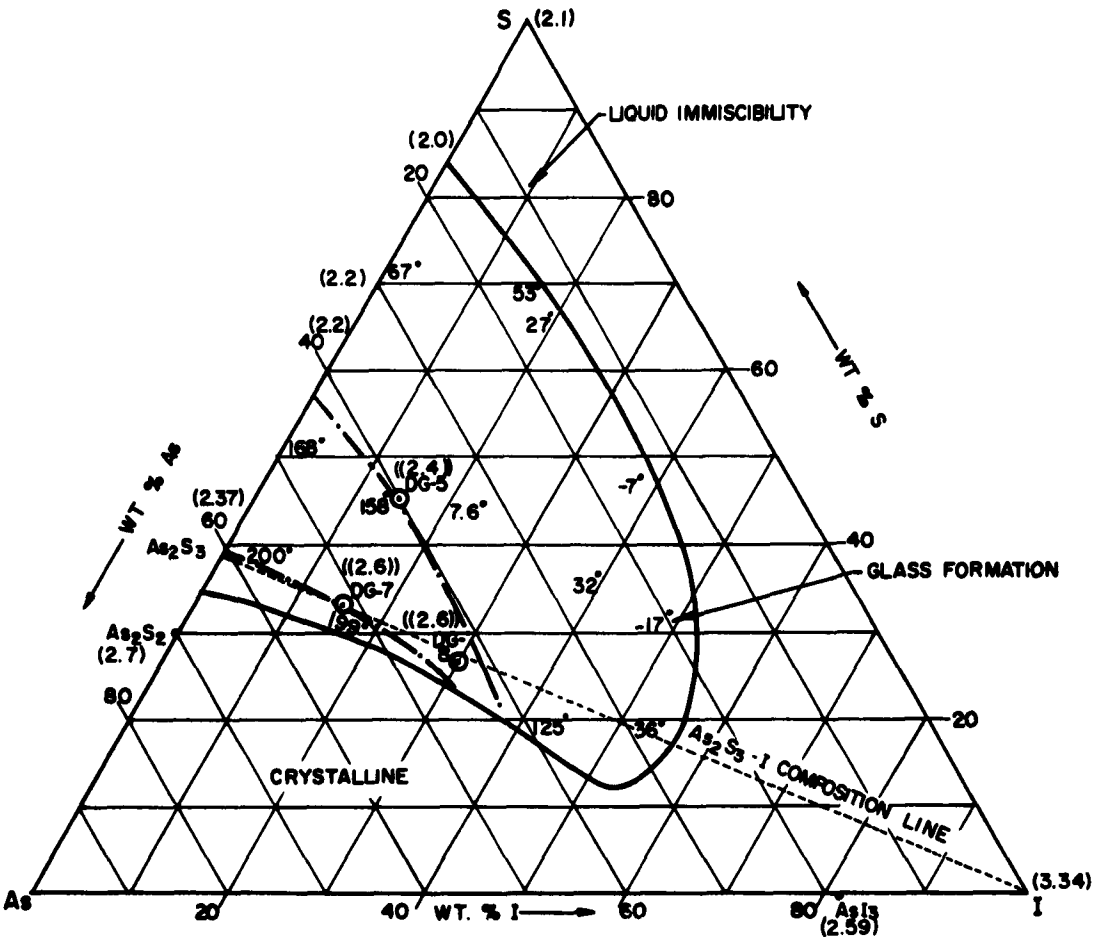

Fig. 26. The phase diagram of the As-S-I system shows the glass forming regions,[55] softening points in °C,[55] and indices of refraction. The indices of refraction enclosed ( ) are from refs. 53, 56, 60 and those enclosed (( )) are ones measured for material synthesized here.

better results are obtained by the use of an evacuated, quartz ampoule which is heated with the reactants at 500 to 600° C for periods up to 24 hours.

The indices of refraction for the compositions for which they have been determined have been plotted on the triangular-coordinate compositional diagrams (Fig. 25, 26) in order to obtain some estimate of the index of refraction for an intermediate composition. It is evident that reasonably suitable compositions are available.

Although it has been found that As-S-Br and As-S-I glasses adhere well to As_2S_3 light pipes, these inorganic glasses did not prove to have sufficient adherence to silicon or silicon oxide to allow fabrication of strong assemblies. For light pipe 1/16 inch in diameter a passable assembly could be achieved. However, for 12-mil-diameter light pipes it was necessary to hold an assembly together under pressure.

Nevertheless, until a material which is more suitable from the mechanical standpoint can be found, these optically appropriate glasses must serve the purpose. Polymers such as the epoxies with an index of refraction of about 1.58 provide a good assembly but their low refractive index is a serious impediment to good light transfer.

4. LIGHT-COUPLED DEVICES

A light-coupled device is one in which the input and output circuits are electrically isolated: Electrical coupling is accomplished entirely by means of the light which passes between the two circuits. Light-coupled transducers have been constructed with p-n-junction light sources and with photodiode and photo-transistor receivers. The coupling between the input and output has been achieved by means of a light-pipe, the theory and practice of which have been discussed in Section 3. In addition, a light-operated flip-flop has been made to demonstrate an opto-electronic functional device of the sort that would be encountered in an optically-coupled computer.

Transducers

In order to demonstrate the principle of optical coupling and to obtain data on the current-transfer coefficients ξ_f and ξ_r which could be achieved for the forward and reverse directions of input current, respectively, light-coupled transducers were constructed with XLD-3(100d) diodes as the transmitting and receiving elements. The forward-current-transfer coefficient may be estimated for a Pyrex light pipe as follows: The diodes chosen, XLD-3(100dp .25) and XLD-3(100dn .068), had an efficiency of $\geq 6 \cdot 10^{-6}$ outside of the oxide (Tables I and II) which corresponds to $\geq 2 \cdot 10^{-4}$ photons per electron over 2π steradians internally. The receiver efficiency at a wavelength of 1.1 microns was found to be about 6%. Then the available forward-current-transfer coefficient ξ_f

would be $2 \cdot 10^{-4} \cdot 6 \cdot 10^{-2} = 1.2 \cdot 10^{-5}$. The values of ξ_f observed with IR 20 and As_2S_3 light pipes (Table VII) are two orders of magnitude or more lower than the maximum. The large transfer of 0.206 (p. 70) which would be expected for an As_2S_3 light pipes has not been achieved because of interface losses in the presence of the epoxy cement with a low refractive index between the light pipe and the silicon diodes. These considerations were examined in additional detail in light-coupled transducers which were constructed with a phototransistor as the receiving element.

In the light-coupled transducers which use Amelco TA-44 type transistors of circular geometry and TA-44 transistors of star geometry the input diode was the emitter-base junction of the transistor; the output unit was operated as a phototransistor with the base floating. The output phototransistor was selected for $\beta \geq 100$ for 10^{-5} A collector current and for $I_{CEO} < 10^{-8}$ A at 22.5 V. The time constants of these transducers were predominantly determined by the phototransistor because even with forward-current operation the emitter-base-junction light source showed a radiative-recombination lifetime $< 2 \cdot 10^{-7}$ sec. The phototransistor time constant in the manner used was primarily determined by the time constant of the emitter-base-junction capacitance. For purposes of comparison, the light-coupled-transducer, current-transfer coefficients have been normalized to a time constant of 30 microsec and to a light-pipe area corresponding to a 30-mil-diameter pipe (Table VIII). These light-coupled transducers generally show nearly linear output-vs-input-current characteristics over nearly two decades of current (Figs. 27 and 28).

Table VII. The current-transfer coefficients for light-coupled transducers constructed with XLD-3(100d)-type diodes evaluated at about 1 A forward current and about $\frac{1}{2}$ A reverse current. A reverse-bias voltage of 6 V was used on the receiver diode; with a load resistance of 820 k the time constants were about 50 microsec.

Diodes	Light Pipe				
XLD-3(100d ...)	Material	Diameter (mils)	Length (inch)	ξ_f	ξ_r
p. 25	As_2S_3	12	0.75	$4.7 \cdot 10^{-8}$	$1.5 \cdot 10^{-8}$
n. 068	As_2S_3	12	0.5	$4.2 \cdot 10^{-8}$	$2.1 \cdot 10^{-8}$
n. 068	As_2S_3	12	0.5	$2.7 \cdot 10^{-8}$	$8.7 \cdot 10^{-9}$
n. 068	As_2S_3	12	0.5	$4.2 \cdot 10^{-8}$	$1.5 \cdot 10^{-8}$
p. 25	As_2S_3	30	0.5	$5.1 \cdot 10^{-8}$	-
p. 05	As_2S_3	12	0.25	$7.35 \cdot 10^{-8}$	$1.55 \cdot 10^{-8}$
p. 05	As_2S_3	12	0.205	$1 \cdot 10^{-7}$	-
p. 25	IR 20	12	0.5	$3.9 \cdot 10^{-8}$	$1 \cdot 10^{-8}$

Table VIII. The current-transfer coefficients $\tilde{\xi}_f$ and $\tilde{\xi}_r$ for light-coupled transducers using phototransistors reduced to a time constant of 30 microsec, an input current of 1 A, and a light pipe diameter of 30 mils.

Unit No.	Light Pipe Material	Light Pipe Diameter	$\tilde{\xi}_f$	$\tilde{\xi}_r$
1	Pyrex	30 mils	$7 \cdot 10^{-8}$	$3 \cdot 10^{-7}$
2	Pyrex	30	$7 \cdot 10^{-8}$	$3 \cdot 10^{-7}$
3	As_2S_3	67	$1 \cdot 10^{-6}$	$4 \cdot 10^{-7}$
4	IR 20	30	$1.5 \cdot 10^{-6}$	$1.1 \cdot 10^{-6}$

The increase in the current-transfer coefficients of units No. 3 and 4 over No. 1 and 2 (Table VIII) is partly a consequence of the change to light pipes with a higher index of refraction and partly to a change to star from circular geometry phototransistors.

The low values of current transfer observed for the light-coupled transducers is primarily a consequence of the presence of silicon dioxide and epoxy cement between the silicon and the light pipe. For example, the light transfer through an As_2S_3 light pipe between silicon

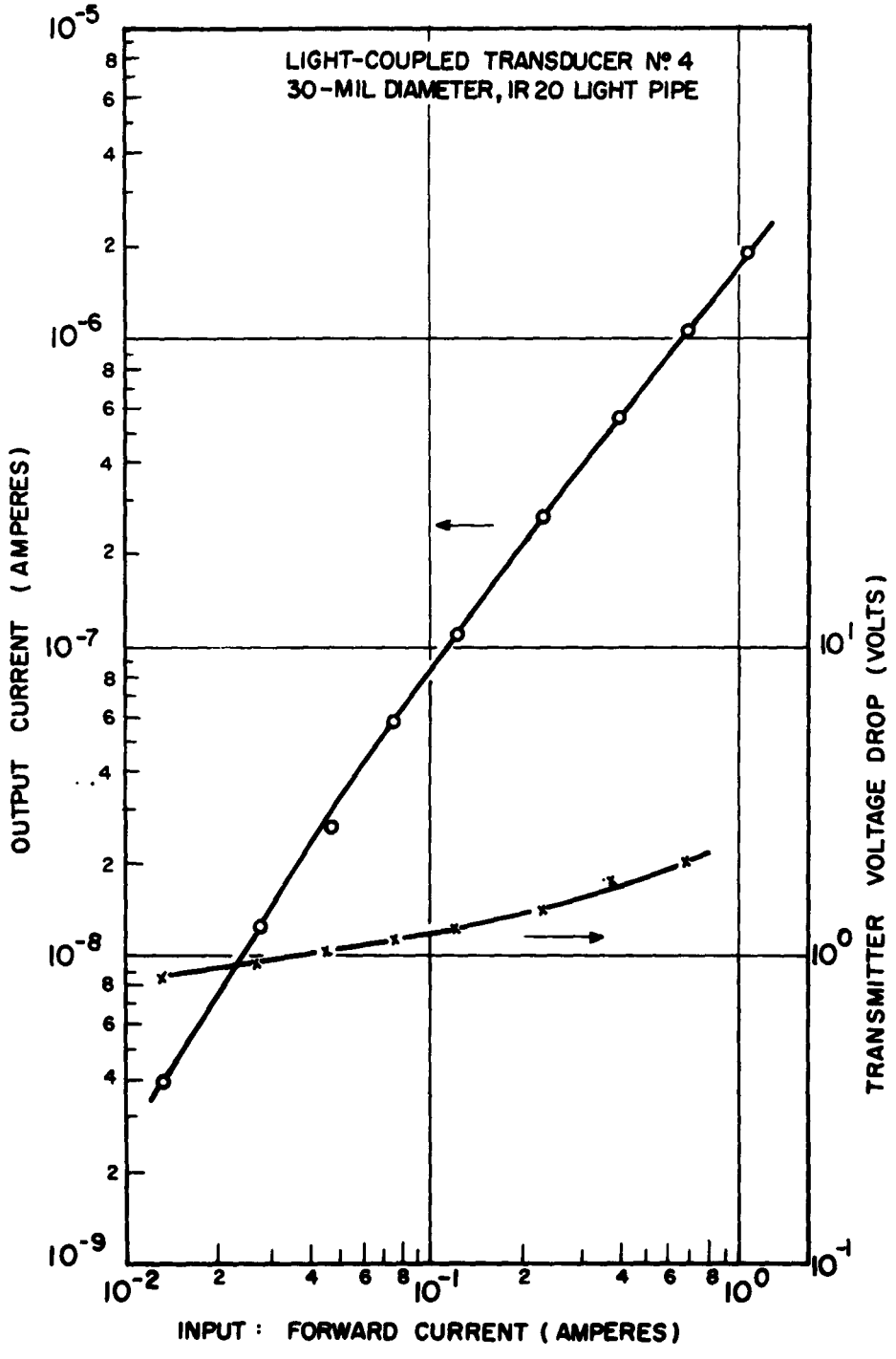

Fig. 27. Output current vs forward input current for light-coupled transducer No. 4 with a 30-mil-diam light pipe of IR 20.

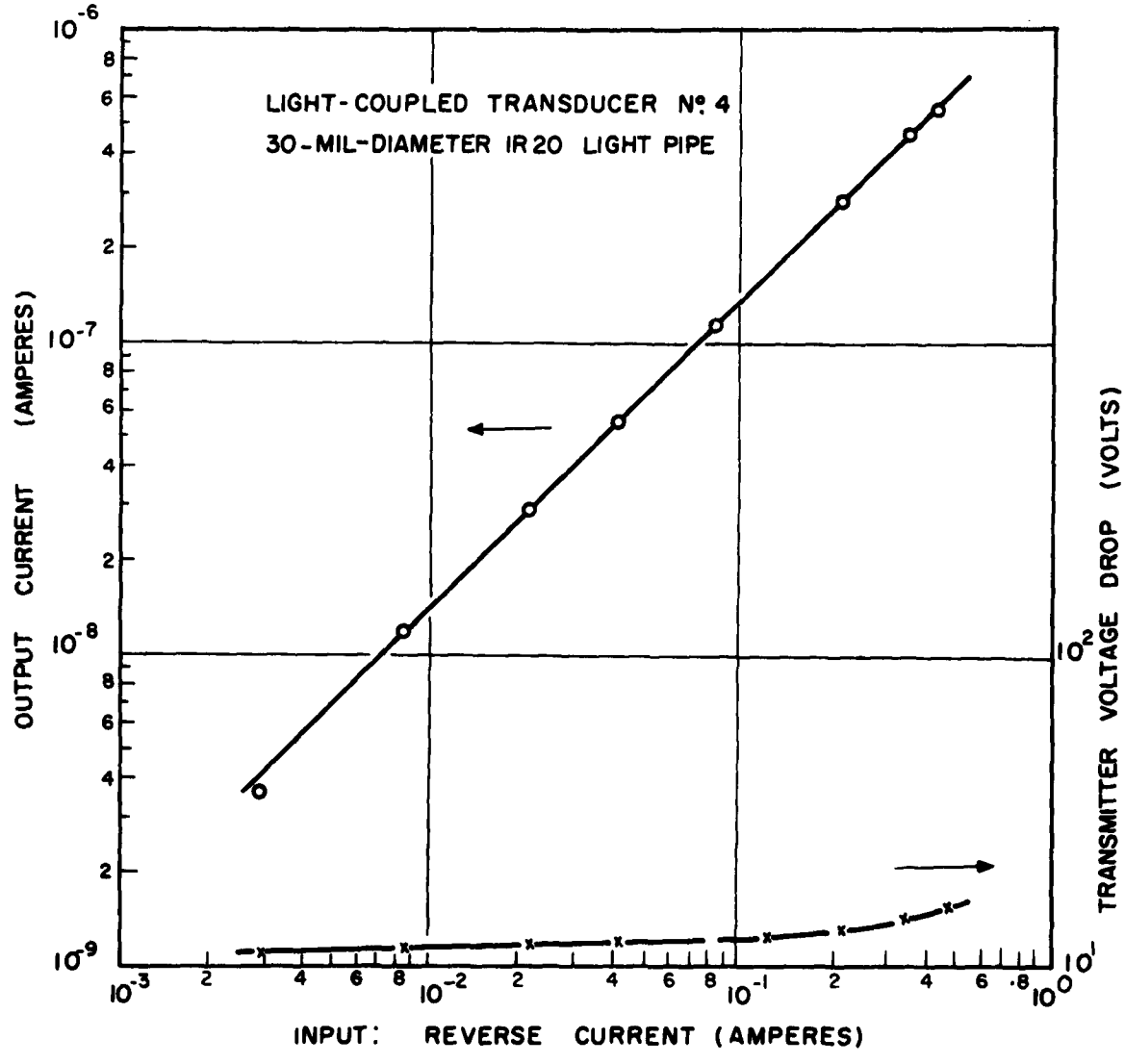

Fig. 28. Output current vs reverse input current for light-coupled transducer No. 4 with a 30-mil-diam light pipe of IR 20.

devices was calculated to be 0.206. However, if epoxy cement with $\underline{n} = 1.58$ intervenes, the loss from multiple reflections yields a transmission of 0.82 (p. 70 ff.). In addition, the fraction of the radiation which is emitted from silicon into epoxy is about 0.10 of that available and an As_2S_3 light pipe accepts about 0.41 of this radiation Therefore, the overall light transfer would be $(0.82)^2 \cdot 0.1 \cdot 0.41 = 0.028$ or about 14% of the transfer of 0.206 achievable with an As_2S_3 light pipe.

With an available current-transfer-coefficient of 10^{-5} for a diode pair the overall transfer with an As_2S_3 light pipe attached with epoxy cement would be about $3 \cdot 10^{-7}$ which has been nearly achieved with a short light pipe (Table VII). With an IR 20 light pipe attached with epoxy cement the performance would be poorer. The decrease of current transfer with increase of length of the light pipe (Table VII) may be attributed to the absorption of light in the As_2S_3, to scattering of the light by internal bubbles, stones, and striae, and to reflection losses incurred by surface imperfections.

An Optically-Actuated Flip-Flop

In a further test of the feasibility of optical interconnection of electronic circuits an Amelco microcircuit flip-flop was taken from a

production run. This unit is made on a silicon chip about 50 x 50 mils in size. A light pipe of 12-mil-diameter As_2S_3 was attached with epoxy cement over the base of the input transistors (Fig. 29). A gallium arsenide diode was used as a light source because preliminary measurement had indicated that the operation of the unit with a silicon p-n-junction light source would not be feasible without an additional stage of amplification, i.e. a phototransistor preceding the flip-flop.

The gallium-arsenide diode was made on material doped n-type with tellurium to a charge carrier number density of about $2 \cdot 10^{17}$ cm^{-3}. The junction was formed by closed-tube diffusion from zinc vapor. The diodes were mounted with the flat, n-type region cemented against the light pipe with epoxy resin. Measurements of the light output of these diodes with the 7102 photomultiplier showed an internal efficiency for these diodes which was estimated to range from $3.5 \cdot 10^{-3}$ to $2.2 \cdot 10^{-2}$ photons per electron at room temperature.

The circuit in which the flip-flop was used (Fig. 30) was provided with adjustable bias to reduce to a reasonable value the photocurrent required to trigger it. Operation was achieved with currents ranging from 0.3 to 1 A through the gallium-arsenide diode. The length of light pulse required to trigger the flip-flop ranged from 200 to 800 nanosec depending on the bias adjustment and the current through the light-source diode. The flip-flop when operated under the design conditions has a delay time of about 30 nanosec. Any possibility of electrostatic coupling between the input circuit and the flip-flop was minimized by means of a shield can placed over the TO-5 header on which the flip-flop was mounted; the light pipe emerged through a hole in the can.

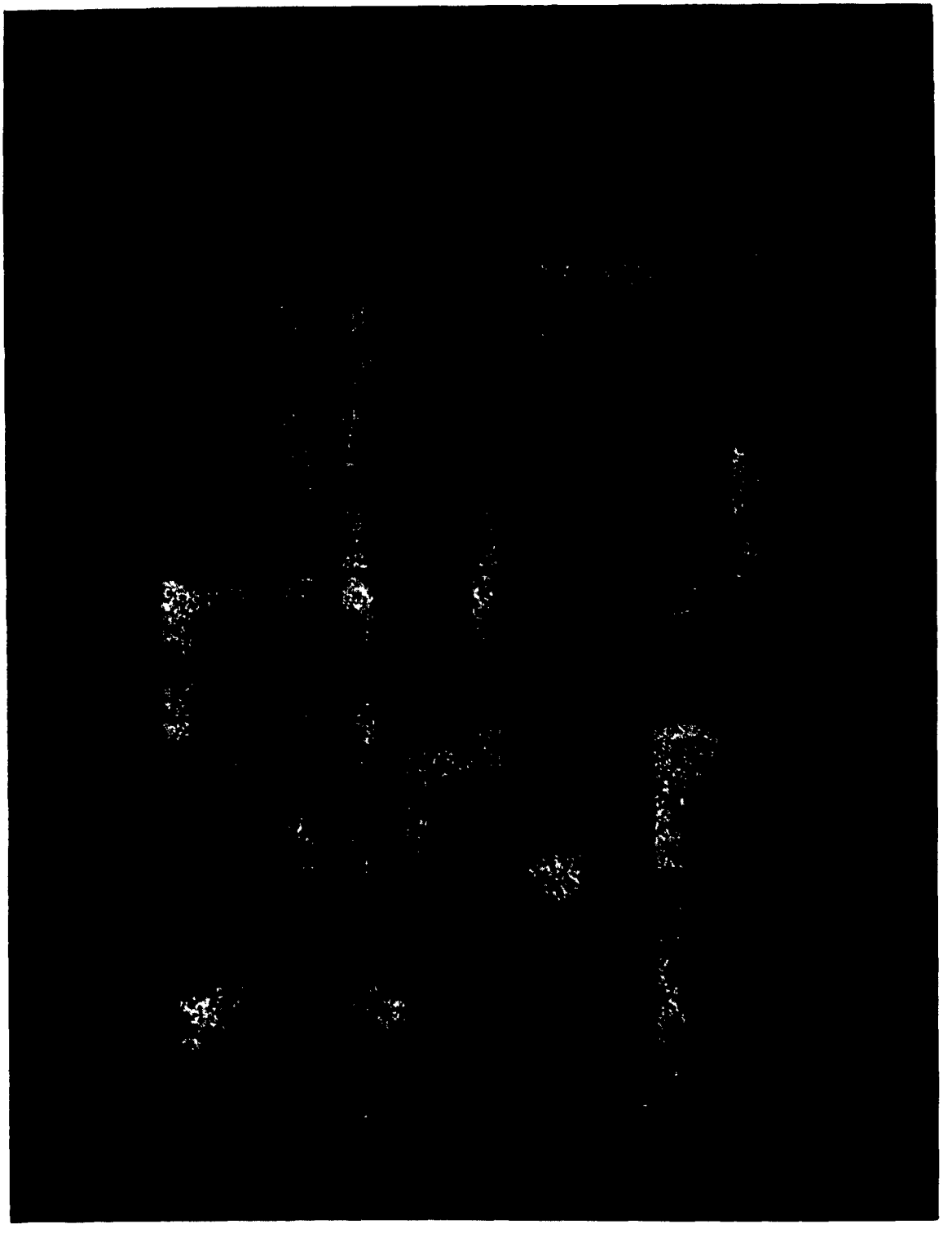

Fig. 29. A photomicrograph of a microcircuit flip-flop at about 135X magnification with the location of the 12-mil-diameter light pipe shown.

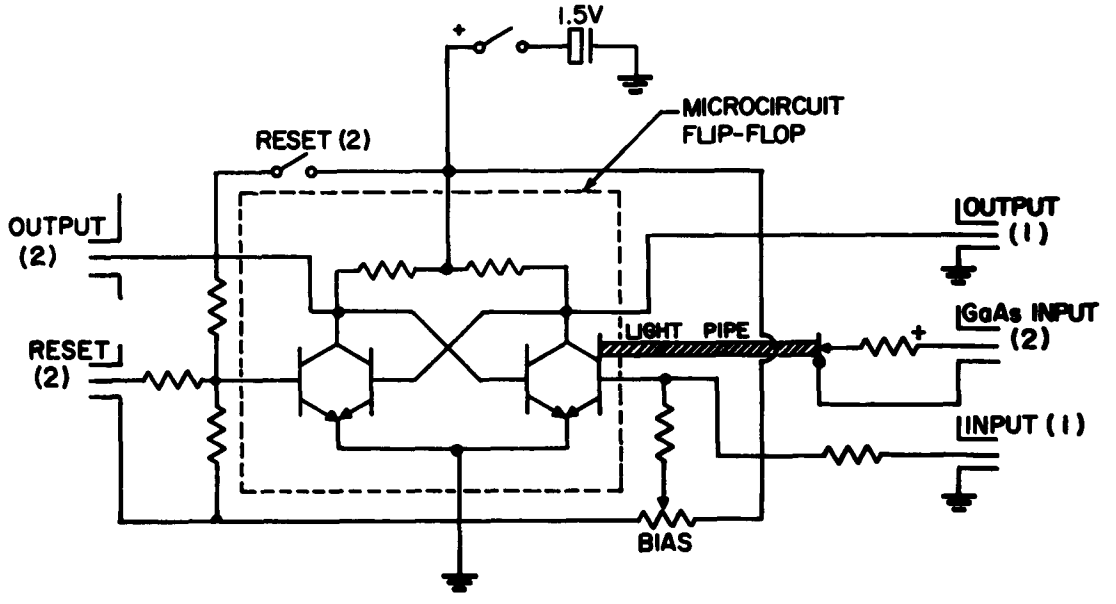

Fig. 30. The opto-electronic circuit with a microcircuit flip-flop which was arranged for optical actuation by means of light through a light pipe from a GaAs diode in a second, electrically-isolated circuit.

5. EPITAXIAL LIGHT SOURCES

Relatively poor efficiency of light production has been achieved in silicon p-n junctions in comparison with that which has been achieved with gallium arsenide and with gallium arsenide-phosphide material. On the other hand, the state of the art of microcircuitry is far advanced for silicon as the substrate, whereas it is almost unknown for a gallium-arsenide substrate. Therefore, a device which could combine the chief merits of both materials on one substrate would be of great value in optoelectronics.

The lattice constant of gallium phosphide (5.45 Å) is very close to that of silicon (5.43 Å) so that the possibility of epitaxial growth of the former on the latter might be feasible in this respect. Epitaxial gallium phosphide would not provide as highly efficient an electroluminescent material as gallium arsenide. However, it has been shown that alloys of composition $Ga(As_{1-x}P_x)$ for $x < \frac{1}{2}$ can also be readily grown by epitaxial methods and that these compositions yield light with an efficiency comparable to that for GaAs ($x = 0$).[61, 62] Therefore, once epitaxial GaP has been obtained on silicon the composition of the

---

[61] N. Holonyak, Jr., and S. F. Bevacqua, Appl. Phys. Letters 1, 82 (1962).

[62] J. W. Allen and M. E. Moncaster, Phys. Letters 4, 27 (1963).

layer could be graded to that of an efficient electroluminescent material; or, possibly, the proper composition might be put down in the first place.

Experiments have been made in which GaP would be deposited by vapor transport on silicon. Iodine vapor has been employed with polycrystalline GaP (Merck) as the source and a silicon wafer as the substrate in a closed tube at about 950° C.[63] Some evidence was obtained for a small deposit of GaP on Si but the results were not conclusive.

The open-tube experiments were carried out after the manner of Ing and Minden[64] for GaAs. Purified hydrogen was bubbled through PCl_3 and the vapor was passed over gallium at 1000° C, thence over silicon wafers at 700 to 800° C. The results of these experiments were also inconclusive, though some deposits were obtained.

Evidently the conditions for the epitaxial growth of GaP on Si differ substantially from those suitable for GaAs as a substrate and a more lengthly search will be required.

In addition to experiments performed at Amelco, the Monsanto Chemical Co., via Dr. R. A. Ruehrwein, and Merck and Co., via Dr. T. S. Benedict, kindly cooperated in an effort to obtain the epitaxial

---

[63] A. S. Roy, J. Electrochem. Soc. 109, 751 (1962).

[64] S. W. Ing, Jr., and H. T. Minden, J. Electrochem. Soc. 109, 995 (1962).

gallium phosphide on silicon. Their results have thus far been negative. Nevertheless, confidence remains high among all concerned that the material required can be produced.

6. CONCLUSIONS AND RECOMMENDATIONS

The experimental data have shown that silicon p-n junctions are versatile sources of radiation. However, the experiments have also shown that the efficiency of production of radiation in silicon at its present state is perhaps two orders of magnitude lower than that which has been achieved in gallium arsenide and the like. Although forward-current radiation is that most efficiently produced in silicon, the time constants of the radiative process tend to be long and to increase with increasing efficiency which places a serious limitation on this mode of operation for high-speed applications. Also the impedance of a forward-current junction radiator tends to be low (perhaps 1 to 2 milliohms cm^2 at 10^3 A cm^{-2}).

A silicon p-n junction operated on reverse current provides a lower efficiency but, perhaps, the highest-speed, semiconductor light source available. The spectrum is very broad (about 3 eV) in contrast to the forward-current spectrum (about 0.3 eV at room temperature) when even very weak radiation is considered. The impedance of a reverse-current-operated junction may be one to two orders of magnitude greater than for the same junction operated on forward current. However, as far as power efficiency is concerned, the higher impedance is a disadvantage.

The origin of both forward and reverse-current radiation is incompletely understood. The long-wavelength component ($\lambda \simeq 2.2$

microns) may be attributed to intraband transitions of hot holes, as in germanium, though the possibility of hot-electron, intraband transitions should also be considered for silicon. A more thorough understanding of this radiation could lead to the achievement of more efficient generation of radiation by such means.

Although negative results were obtained in the experiments which were undertaken to generate radiation by recombination at neutral-indium impurity atoms in silicon following the work of Pokrovsky and Svistunova,[15] the significance of their work should not be dismissed. Further research on the production of radiation with a probability of nearly one for radiative recombination as they reported is important because it could lead to new understanding of efficient processes for the production of radiation in semiconductors. Also such processes are of utmost importance to optical-maser (laser)type devices.

The light-pipe method of optically interconnecting electrical circuits has been demonstrated in theory and practice. The extension of this method to large, planar arrays of devices by means of a fiber-optic plate for light coupling follows immediately. However, the technique of achieving satisfactory contact between materials with a high refractive index needs to be perfected. Until this technique is mastered, any large-scale, opto-electronic device is impracticable.

Aeronautical Systems Division, AF Avionics Laboratory, Electronic Technology Division, Wright-Patterson AFB, Ohio.
Rpt Nr ASD-TDR-63-606, PHOTRONICS: The Generation of Light in Silicon P-N Junctions and the Optical Coupling of Semiconductor Devices. Final Report, July 63, 104 p. incl illus., tables, 64 refs. Presented at AGED-DOD Microelectronic Device Conference, Durham, N. C., May 63.

Unclassified Report

(over)

1. Semiconductor device
2. Electroluminescense
3. Optical coupling
4. Fiber optics
5. Microminiaturization

I. AFSC Project 4159, Task 415910
II. AF 33(657)-8678
III. Amelco, Inc., Mountain View, California
IV. Gilleo, M. A.
V. Not aval fr OTS
VI. In DDC collection

The coupling of electrical circuits by optical means was investigated. The speed and efficiency of forward and reverse-current radiation from silicon p-n junctions were evaluated as a function of resistivity of the base material and of the depth of diffusion. A light-pipe coupling element was studied in theory and experiment. Light-coupled transducers were constructed. An optically-actuated, silicon, microcircuit flip-flop was made with an As_2S_3 light pipe and a GaAs diode as the light source.

Aeronautical Systems Division, AF Avionics Laboratory, Electronic Technology Division, Wright-Patterson AFB, Ohio.
Rpt Nr ASD-TDR-63-606, PHOTRONICS: The Generation of Light in Silicon P-N Junctions and the Optical Coupling of Semiconductor Devices. Final Report, July 63, 104 p. incl illus., tables, 64 refs. Presented at AGED-DOD Microelectronic Device Conference, Durham, N. C., May 63.

Unclassified Report

(over)

1. Semiconductor device
2. Electroluminescense
3. Optical coupling
4. Fiber optics
5. Microminiaturization

I. AFSC Project 4159, Task 415910
II. AF 33(657)-8678
III. Amelco, Inc., Mountain View, California
IV. Gilleo, M. A.
V. Not aval fr OTS
VI. In DDC collection

The coupling of electrical circuits by optical means was investigated. The speed and efficiency of forward and reverse-current radiation from silicon p-n junctions were evaluated as a function of resistivity of the base material and of the depth of diffusion. A light-pipe coupling element was studied in theory and experiment. Light-coupled transducers were constructed. An optically-actuated, silicon, microcircuit flip-flop was made with an As_2S_3 light pipe and a GaAs diode as the light source.